Transgenic complementation of *rumpshaker* with wild type Proteolipid protein

A thesis presented to The Faculty of Veterinary Medicine
University of Glasgow

for the degree of Master of Science

Jennifer Ann Barrie

March 2008

Abstract

Mutations in the x-linked myelin proteolipid protein 1 gene (*PLP1)* cause the heterogeneous syndromes of Pelizaeus Merzbacher disease (PMD) and Spastic paraplegia type 2(SPG2) in man (Hudson et al., 2004). A single base change mutation in our spontaneous mouse model *rumpshaker* (*Plp*$^{jp\text{-}rsh}$*)(*Ile^{186}Thr) (Schneider et al., 1992) generates a misfolded protein resulting in dysmyelination and increased numbers of apoptotic oligodendrocytes. The phenotype varies from mild on the original C3H background to lethal when backcrossed onto the C57BL/6 mouse strain (Al-Saktawi et al., 2003). Utilising the more severe variant we sought to ameliorate the lethal phenotype by transgenic complementation with wild type *Plp1* (Readhead et al., 1994) to normalise the levels of proteolipid protein (PLP) and it's smaller isoform DM20.

The presence of the wild type protein improves the survival of the mice, decreases oligodendrocyte apoptosis and restores normal periodicity to the myelin, however hypomyelination remains severe. Although the PLP/DM20 level is restored to normal the level of myelin basic protein remains low. In addition the presence of the wild type protein does not ameliorate the unfolded protein response induced by the *rumpshaker* PLP/DM20.

Dedicated with love to the memory of my parents Margaret and Willie Scott

List of Contents

.

List of Figures

List of Tables

Acknowledgement

I would like to thank my supervisor, Prof. Ian Griffiths, for his guidance and support during this project. I would also like to express my gratitude to Dr Mark McLaughlin for his invaluable instruction, advice and patience.

Many thanks to the Management Group and Graduate School of The Faculty of Veterinary Medicine for allowing me to undertake this degree.

Thanks also to Professor Klaus-Armin Nave for establishing the *rumpshaker* mutation on C57BL/6NCrlBR background and for donating the line to us. In addition, I would like to acknowledge Prof. Carol Readhead for originally donating the #66 transgenic line of mice.

My appreciation goes to the staff of the General Parasitology Unit of Biological Services for providing excellent care of the animals used in this study.

I would like to acknowledge the help of Prof Ian Griffiths for some of the morphological measurements, Dr Mark McLaughlin for the RT-PCR data and images of CHOP and ATF3 and Dr Paul Montague for his help with the vagaries of molecular biology. I am grateful to Dr. Saadia Karim for performing the quantitative real time PCR and to Douglas Kirkham for the many genotype PCRs he performed.

I would also like to thank Mailis McCulloch, Dr Julia Edgar, and Marie Ward for their help, support and friendship.

Finally to my family, thank you for your love and support, it is much appreciated.

Declaration

I, Jennifer Ann Barrie, do hereby declare that the work carried out in this thesis is original, was carried out by myself or with due acknowledgement, and has not been presented for award or degree at any other university.

1. Introduction

1.1 Area of study

The mammalian nervous system can be divided into two distinct regions, the central nervous system (CNS) and the peripheral nervous system. The *rumpshaker* mutation is a genetic defect primarily affecting the CNS and therefore our study was confined to this area. The CNS itself can be considered as two separate structures, the brain and the spinal cord. The cervical spinal cord in particular lends itself well to quantitative assessment and thus we chose to focus our study on this area.

1.2 Spinal Cord Structure

The spinal cord, although divided along its length into several distinct regions, is essentially composed of central grey matter, containing neurones, glia and blood vessels, and peripheral white matter which can be subdivided into dorsal, ventral and lateral columns (funiculi). The white matter is comprised of myelinated axons interspersed with occasional non-myelinated axons and numerous glia. The glial cell types are astrocytes, microglia and oligodendrocytes. Many precursor (undifferentiated) glial cells can also be found within the white matter.

1.3 The Glia

Glia are the non-neuronal cells of the brain. Over a hundred years ago Ramon y Cahal observed that, given their close association with neurones, they must do more than fill in the spaces. It is only recently that their influence on the functions of the CNS has begun to be discovered.

1.3.1 Glial cell development

Within the developing mammalian brain in an area of the neural tube known as the subventricular zone (SVZ) is found a reservoir of multipotential and lineage restricted progenitor cells formed from the neuroepithelium. These cells migrate dorsally and laterally from the SVZ to populate and form the white matter tracts of the developing spinal cord. Fine control of the migration and differentiation of these progenitor cells is

essential, as the more mature forms cannot migrate. Several signalling molecules and transcription factors are involved in this control such as sonic hedgehog, bone morphogenic protein and the notch pathway (Colognato & ffrench-Constant, 2004))(Barres & Barde, 2000). Following initial migration it is thought that dorsal regions develop the capacity for oligodendrocyte generation (Baumann & Pham-Dinh, 2001).

1.3.2 Astrocytes

Traditionally astrocytes were considered as two main classes, the synapse associated protoplasmic astrocytes found in grey matter and those associated primarily with nodes of Ranvier, the fibrillary astrocytes of the white matter. Current classifications recognise the very heterogeneous phenotype of astrocytes. The astrocyte performs many functions within the mammalian CNS, sequestration and/or redistribution of K^+ during neural activity, removal of glutamate and provision of glutamine for uptake by the neurones, ensheathment of blood vessels contributing to the development and maintenance of the blood brain barrier being among them. Recently however more important functions have been emerging for the astrocyte for example regulation of synaptogenesis and propagation of calcium waves as a means of signalling each other and the surrounding neurones (Nedergaard et al., 2003). In addition, astrocytes have a role in myelination by promoting the adhesion of oligodendrocyte processes to axons (Meyer-Franke et al., 1999). The accepted marker for astrocytes, in both healthy and disease states is Glial Fibrillary Acidic protein (GFAP).

1.3.3 Microglia

Microglia account for around 10% of CNS glia but unlike the other glial cells derive from mesenchymal tissue rather than the neuroepithelium. They serve as the immune cells of the CNS and in response to injury phagocytose cellular debris as well as eliciting an inflammatory response (Stevens, 2003). They are the endogenous macrophages of the CNS and during an insult their numbers can increase due to recruitment from the circulating monocytes. Indeed, endogenous microglia and recruited monocytes are indistinguishable.

1.3.4 Oligodendrocytes

Oligodendrocytes are the myelin-forming cells of the CNS. Each oligodendrocyte produces several processes each of which contacts and wraps around an axonal segment eventually condensing to expel all but a small pocket of cytoplasm at the axonal surface.

1.3.4.1 Oligodendrocyte classification

There have been several methods adopted for the classification of oligodendrocytes. Rio Hortega classified them into 4 categories according to the number of processes (Baumann & Pham-Dinh, 2001). Butt (Butt et al., 1995) also described 4 classes according to their morphology and the size and thickness of myelin sheath formed and Mori and Leblond described 3 types, light, medium and dark, a description of the cytoplasmic density as viewed using electron microscopy (Mori & Leblond, 1970). More recently, an understanding of the various developmental stages in oligodendrocyte lineage has been possible with the discovery of specific biochemical markers and a range of antibodies against them.

1.3.4.2 Oligodendrocyte differentiation

Oligodendrocyte differentiation occurs in a spatial/temporal manner. Early oligodendrocyte progenitor cells (OPCs) migrating from the subventricular zone express platelet derived growth factor receptor α (PDGFαR) and the sulphated proteoglycan NG2. They migrate and proliferate to populate the white matter tracts of the CNS. Late OPCs no longer migrate but still divide. In addition to NG2 and PDGFαR they express 04 and CD9. A few days before myelination the late OPCs differentiate into premyelinating oligodendrocytes, which begin to extend multiple processes. They no longer express NG2 or PDGFαR but do express galactocerebroside (GalC), myelin-associated glycoprotein (MAG), 2',3'-cyclic nucleotide 3' phosphodiesterase (CNP), myelin basic protein (MBP) and DM20 (the minor isoform of proteolipid protein (PLP)). During final differentiation to a myelinating oligodendrocyte the cell becomes polarised and directs myelin proteins to specific membrane domains. MAG is localised to the periaxonal membrane, CNP to non-compact regions of the myelin internode, MBP and the newly expressed PLP are targeted to the compact myelin. However, if the oligodendrocyte should fail to myelinate an axon then it is programmed to die. It has been estimated that as many as 50% of new oligodendrocytes die (Trapp et al., 2004).

1.4 Myelination

Myelination is a process that occurs at varying times in the developing CNS. In the mouse it begins just before birth in a rostrocaudal direction in the spinal cord (caudorostrally in brain) (Schwab & Schnell, 1989) and is not complete in the brain until 45-60 days postnatally. The newly matured oligodendrocytes, upon contact with axons, elaborate sheet

like extensions of their plasma membrane, which spirally wrap the axon and eventually compact to form the myelin sheath. The principal function of this sheath is to allow rapid saltatory conduction of action potentials from the neuronal cell body along the length of the axon. Depending on its location a single oligodendrocyte can enwrap up to 40 segments of axon (Coman et al., 2005), although adjacent myelin sheaths on any given axon are never formed by the same oligodendrocyte.

1.4.1 Myelin morphology

The mature myelin sheath has a distinct periodic structure, with alternating electron light and dense layers. The light layer, the intraperiod line, is formed by the close apposition of the extracellular face of the plasma membrane, whilst the dark layer, the major dense line, is formed by the fusion of the cytoplasmic surfaces of the membrane. The periodicity of the lamellae is ~12nm and each segment of a myelinated axon or internode is 150-200µm in length. Between each internode there is an area of axon lacking a myelin sheath known as the node of Ranvier. Both the thickness of the myelin sheath and the internodal length are positively related to the axonal diameter. Where the myelin lamellae end, at the node of Ranvier, paranodal loops containing oligodendrocyte cytoplasm can be found, this area is called the paranode. Each of these anatomically distinct regions is formed by specific interactions between the axon and the myelinating oligodendrocyte (Baumann & Pham-Dinh, 2001).

1.4.2 Myelin composition

CNS white matter consists of 40-50% myelin by dry weight; it is the major constituent of the white matter. Myelin itself consists of 30% protein and 70% lipid, which is a ratio unique for biological membranes (Baumann & Pham-Dinh, 2001). The lipid content consists of cholesterol, phospholipids and glycolipids. The most common lipids found in myelin are the glycosphingolipids, particularly GalC. There are many myelin proteins, the majority of which are specific to oligodendrocytes and the myelin sheath. Numbered among them are MOG, MOBP, OSP and Cx32, which account for a very small proportion of the myelin proteins. Others have a more distinct role and account for greater proportions.

1.4.2.1 CNP (2',3'-cyclic nucleotide 3' phosphodiesterase)

CNP is only 4% of the total myelin protein. It is localized to the cytoplasm of non-compacted myelin particularly at the paranodal loops and adaxonal cytoplasm. Whilst the exact function of CNP remains elusive it has been postulated that it associates with actin and tubulin components of sub-membranous cytoskeleton where it plays a role in membrane expansion and migration, indeed transgenic mice overexpressing CNP display perturbed myelin formation and abnormal membrane expansion (Trapp et al., 2004). Mice deficient in CNP develop an axonopathy (Lappe-Siefke et al., 2003).

1.4.2.2 MAG (Myelin-associated glycoprotein)

MAG is a type 1 integral membrane glycoprotein that accounts for only 1% of total myelin protein. Two MAG proteins have been identified Large MAG (L-MAG) and small MAG (S-MAG). It is selectively targeted to paranodes and the periaxonal membrane and as such is in direct contact with the axon. L-MAG has been detected in endosomes during early myelination, its endocytosis possibly being mediated by binding to a ligand present in the periaxonal space or the axolemma. Once endocytosed it is transported back to the oligodendrocyte body, a possible mechanism by which the axon influences oligodendrocyte myelination (Trapp et al., 2004).

1.4.2.3 MBP (Myelin basic protein)

Myelin basic protein is one of the major proteins of CNS myelin accounting for 30% of the total myelin protein (Baumann & Pham-Dinh, 2001). It exists in rodents as four main isoforms produced through translation of separate mRNAs generated from alternative splicing of the gene (Campagnoni & Campagnoni, 2004). The molecular masses of these four isoforms are 14, 17, 18.5 and 21.5kDa. The 17 and 21.5 isoforms appear early during mouse development, in fact the *Mbp* gene has been demonstrated in developing mouse embryos as early as E14.5 (Baumann & Pham-Dinh, 2001) *Mbp* mRNA is translocated to the inner tongue of the oligodendrocyte where it is translated and the protein inserted into the myelin sheath (Trapp et al., 2004). MBP plays a major role in myelin compaction adhering to the cytoplasmic leaflet of the myelin bilayer. Electron microscopic studies of the mutant shiverer mouse spinal cord have demonstrated that the major dense line of the myelin is missing. The shiverer mouse has a major defect in the *Mbp* gene in which 5 of the 7 exons are deleted.

In addition to the classic MBP isoforms there exists a group of alternatively spliced proteins from a larger *Mbp* gene, this one consisting of 10 exons, 7 of which code for the classic isoforms. These alternative proteins have been called the Golli-MBPs, their full function has yet to be elucidated, but it has been reported that among other functions they have a role in signalling pathways (Campagnoni & Campagnoni, 2004).

1.4.2.4 PLP (Proteolipid protein) and DM20

Proteolipid protein was discovered by Folch and Lees as early as 1951 (Folch & Lees, 1951). It is the most abundant protein of central nervous system myelin accounting for over 50% of the total. The gene is highly conserved throughout nature and exists as a single copy gene on the X chromosome (Xq22.2 in human). The gene spans 17kb and consists of 7 exons (Diehl et al., 1986; Macklin et al., 1987) with a single promoter region. The gene encodes a 276 amino acid integral membrane protein with a basic isoelectric point (Vouyiouklis et al., 2000). Unusually, alternative splicing occurs within exon 3 to generate PLP and its smaller but distinct isoform DM20. Two very close transcription initiation sites exist (Milner et al., 1985) both of which are used. During peak myelination most transcription initiates from the upstream site and the full length PLP is expressed, however during oligodendrocyte development when transcription initiates from the downstream site DM20 is selectively expressed.

Regulation

PLP1 gene expression is regulated by the balance between activators and repressors, which bind to sites in the gene. It is likely that some of these transcription factors will recognise other myelin gene promoters as a mechanism for co-ordinately controlling groups of genes via common DNA sequences or cis elements.

Conservation

PLP/DM20 are part of the Proteolipid gene family the lipophilins (Gow, 1997) featuring 4 transmembrane domains with intracellular termini, a large extracellular loop between transmembrane domains 3 and 4 and an intracellular domain between 2 and 3 (Figure 1.). All family members have a high degree of amino acid conservation.

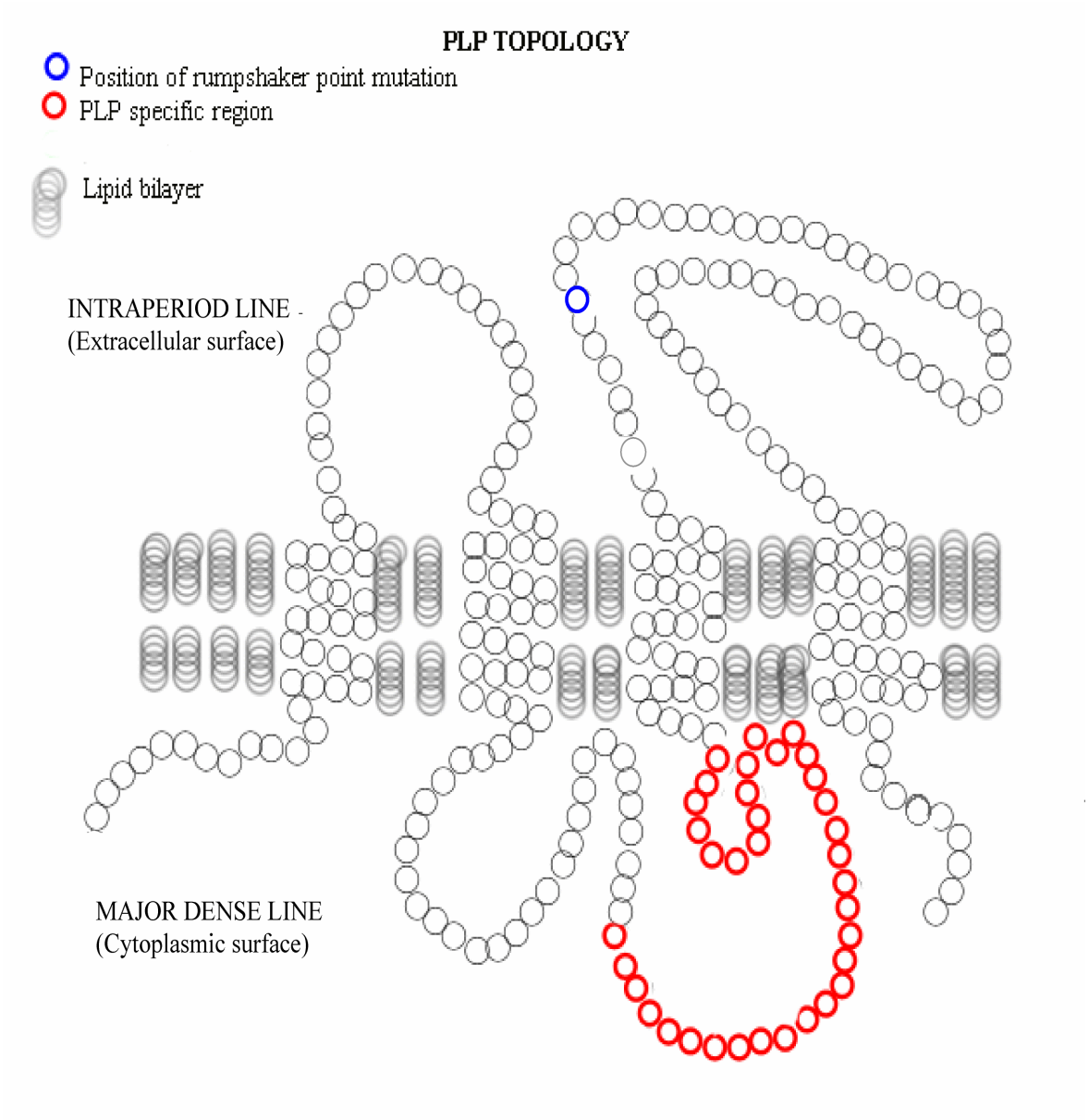

Figure 1. Schematic of predicted topology of PLP/DM20 protein within the lipid bilayer of the oligodendrocyte plasma membrane, showing four transmembrane domains, a large extracellular loop between domains 3 and 4 and an intracellular loop between domains 2 and 3, both termini are intracellular. Adapted from (Garbern, 2007)

Translational and posttranslational regulation

The orientation of PLP and DM20 in the rough endoplasmic reticulum is such that both the amino and carboxy termini are exposed to the cytoplasm (Gow, 1997). The correct folding of the proteins within the endoplasmic reticulum is essential for their subsequent transport to the Golgi and eventually the cell surface. During transit through the Golgi, PLP becomes associated with lipid rafts. These are microdomains rich in cholesterol and glycosphingolipids, which act as "rafts" for the assembly of a specific set of proteins. The hydrophobic nature of PLP/DM20 is enhanced by the attachment of long chain fatty acids to the cysteine residues via thioester linkage, the most common fatty acid being palmitate. A further posttranslational modification is proteolytic cleavage at the intracellular loop, thus creating an amino terminal half and a carboxy terminal half (Hudson et al., 2004).

Function of PLP and DM20

Investigations of expression patterns have revealed that DM20 is expressed primarily in pre myelinating oligodendrocytes (Dickinson et al., 1997) and other non-myelinating cells (non-myelin-forming Schwann cells, olfactory nerve ensheathing cells, and myocardial cells). The fact that DM20 expression does not coincide with myelin formation was the first clue that DM20 was distinct from PLP. 'Loss of function mutants' are the most useful tools for investigating the function of PLP/DM20. Genetic manipulation of the *Plp1* gene produced mice lacking PLP/DM20 as well as a line lacking only the PLP isoform. Both transgenic lines manage to elaborate a myelin sheath although in each case the sheath displays abnormal periodicity. The mice lacking both PLP and DM20 have a perturbation of the intraperiod line (Yool et al., 2002) while the mice expressing only DM20 may have an expanded periodicity (Hudson et al., 2004) and pockets of cytoplasm throughout the compact myelin. Given that PLP has 3 fatty acid attachment sites in the intracellular loop whereas DM20 only has one may explain a role for PLP in stably linking adjacent membrane bilayers through intercalation of the fatty acid sites into the opposing bilayer leaflet (Hudson et al., 2004), a function that cannot be replaced by DM20. In each model oligodendrocyte development is normal. In other models, oligodendrocyte death occurs when mutation of the *Plp1* gene results in the translation of a misfolded protein, whereas knockout mice lacking functional PLP develop axonal swellings later in life despite elaborating a relatively normal myelin sheath (Griffiths et al., 1997). The swellings contain mitochondria and other membranous organelles and are associated with a deficiency in axonal transport (Edgar et al., 2004). These findings point to an important role for PLP in the maintenance and survival of axons.

1.4.3 PLP1 Mutants

The *proteolipid protein1* gene encodes the major protein of CNS myelin. Mutations within the gene vary from deletion to missense mutations to additional copies of the gene. The most common feature of the pathology of the mutants tends to be hypomyelination.

1.4.3.1 Mutations in man

Pelizaeus-Merzbacher Disease (PMD), an X-linked dysmyelinating leukodystrophy and the less severe Spastic paraplegia type 2 (SPG2) are associated with mutations of the *PLP1* gene (Inoue, 2005). To date, many mutations have been identified and by far the most common is duplication of the region harbouring the *PLP1* locus. This type of mutation along with null mutations tends to be associated with the milder form of the disease whereas point mutations, of which there are many, are identified with more severe disease states (Yool et al., 2000). Investigation of the pathophysiology of PMD and SPG2 has been aided by the existence of various naturally occurring and engineered animal models

1.4.3.2 Spontaneous disease models in animals

Many spontaneous point mutations of the *Plp1* gene have been described in mice. The *jimpy* mutation (Plp^{jp}), the first to be described, has a point mutation within intron 4 leading to the absence of exon 5 from the mature transcript. The *jimpy-4J* ($Plp^{jp\text{-}4j}$) model harbouring a point mutation in exon 2 is the most severe of the *Plp1* mutations and in these animals death occurs around postnatal day 24. A further *jimpy* mutation the *msd* ($Plp^{jp\text{-}msd}$) has also been described, in these animals the point mutation in exon 7 means that the carboxy terminus is maintained and the phenotype is almost indistinguishable from the classic *jimpy* with death occurring around 3-4 weeks of age. These mutants display acute neurological dysfunction due to lack of a functional myelin sheath. The myelin deficient rat ($Plp^{md)}$) is an example of a spontaneous mutation in a different species. Each is a useful model for investigations of the severe connatal form of PMD. (Nave & Griffiths, 2004)

Investigations of the mild forms of PMD and SPG2 are aided by work on the *rumpshaker* mouse ($Plp^{jp\text{-}rsh}$), the *paralytic tremor* rabbit (Plp^{pt}) and the *shaking pup* (Plp^{sh}). These mutants have less severe phenotypes and although hypomyelination is still a feature, oligodendrocyte numbers are maintained and the animals survive into adulthood (Yool et al., 2000). Interestingly the *rumpshaker* point mutation, Ile-186-Thr, when expressed on the C57Bl/6 background dramatically alters from the mild phenotype to that of a lethal

phenotype. The modifying gene/s responsible for this dramatic change are presently unknown, (Al-Saktawi et al., 2003) however a dramatic increase in apoptotic oligodendrocytes, microglia and a significant drop in the amount of myelin are reported. This same point mutation has been identified in a family with a history of SPG2 (Naidu et al., 1997)

1.4.3.3 Engineered models in animals

Transgenic mice harbouring increased copies of the *Plp1* gene have been generated. The #66 line has 7 copies per haploid genome, #72 has 3 copies per haploid genome (Readhead et al., 1994), and the 4e line has 2. In these mice phenotypic severity closely mirrors copy number with phenotypes ranging from severely dysmyelinated in the high copy number line to normal myelination with late onset demyelination in lines with low copy number. Axonal swellings in later life are also a feature of these duplication mutants. (Anderson et al., 1998)

Additionally, there are two engineered mouse lines with functionally null alleles of the *Plp1* gene, *Plp-null* and Plp^{tmkn1}. Surprisingly these models elaborate large amounts of myelin, have normal numbers of oligodendrocytes and display no obvious clinical phenotype until late in life. (Anderson et al., 1998)

1.5 Transgenic complementation as a rescue strategy

Transgenic complementation has been used to study various myelin mutants. Readhead et al rescued the *shiverer* phenotype by transgenic complementation with a cosmid transgene containing the entire *Mbp* gene (Readhead et al., 1987), Kimura et al subsequently showed that complementation with only one isoform of *Mbp* can restore myelination in the *shiverer* (Kimura et al., 1989). In a further study, Readhead attempted to rescue the *jimpy* phenotype by transgenic complementation with autosomal copies of the mouse wild type *Plp1* gene. The survival and myelination status of the complemented *jimpy* mice was not improved but the number of apoptotic glia was significantly decreased. They also discovered that myelination is extremely sensitive to over expression of the *Plp1* gene as the lines of transgenic mice (#66 and #72 lines) generated to supply the *Plp1* gene for the complementation developed dysmyelination (Readhead et al., 1994). Nadon generated transgenic mice that expressed either the *Plp* or *Dm20* cDNAs in order to study the effect of these individually, when bred on to the *jimpy* phenotype. They discovered that alone

neither had any significant affect, but when both were expressed in *jimpy* partial rescue was achieved (Nadon et al., 1994).

1.6 Aims

As described previously the *rumpshaker* mutation expressed on the C57BL/6 background has a lethal phenotype with death occurring around postnatal day 30. Severe dysmyelination, high numbers of apoptotic oligodendrocytes and increased numbers of microglia are prominent features of this mutant. This study sought to normalise the level of PLP/DM20 by transgenic complementation with wild type *Plp 1* and investigate the effect this has on apoptosis and myelination in addition to the possibility of ameliorating the lethal phenotype

It is not clear if a lack of functional myelin leading to a breakdown of the normal axon/glial interaction and therefore a lack of essential trophic factors is responsible for oligodendrocyte apoptosis, or if the misfolded PLP accumulating in the endoplasmic reticulum causing activation of the unfolded protein response leads to eventual cell death. The study examines the effect of normalised PLP on the UPR in an attempt to understand the cause of cell death.

2. Materials and methods

2.1 Animals

Mice were bred in the General Parasitology Unit animal house of Biological Services, University of Glasgow under licence from the UK Home Office.Animal studies were approved by the Ethical Committee of the Faculty of Veterinary Medicine, University of Glasgow.

2.1.1 Breeding

To generate the genotypes of interest, female *rumpshaker* heterozygote mice on the C57BL/6 background were mated with C57BL/6males carrying a wild type *Plp1* genomic transgene, line#66 (Readhead et al., 1994). Of the 4 genotypes generated, only male *rumpshaker* mice with or without transgene and the wild type male mice were used in the study.

2.1.2 Genotyping

In order to identify the genotype of each animal a 1cm length of tail was collected post euthanasia and snap frozen in liquid nitrogen

2.1.2.1 Preparation of genomic DNA

Digestion was performed by the addition of Nuclei Lysis solution (Promega) containing 0.35mg Proteinase K and 0.1M EDTA at 55˚C. Following complete digestion the protein component was precipitated by the addition of protein precipitation solution (Promega) and the supernatant containing the DNA removed to a microtube containing 2-propanol (Sigma) which upon gentle inversion precipitates the fine threads of DNA. The fine strands of DNA were pelleted by centrifugation and the 2-propanol removed and replaced by 70% ethanol to wash the DNA, which was again pelleted by centrifugation and the 70% ethanol removed. The DNA was allowed to air dry before reconstituting in 100µl DNA rehydration solution (Promega) at 65˚C for 1hour. The DNA was quantified on a Genequant

(Pharmacia Biotech) spectrophotometer and samples prepared at a concentration of 25µg/µl in filter sterilised distilled water.

2.1.2.2 PCR to determine presence of #66 Transgene

To each "ready to go PCR bead"(Amersham Bioscience) 24µl of prepared master mix (0.5µl primer PLP,(sequence 5-CAGGTGTTGAGTCTGATCTACACAAG-3) 0.5µl primer αT7(sequence 5-GCATAATACGACTCACTATAGGGATC-3)(Readhead et al., 1994), 23µl filter sterilized water and1µl(25 µg/ µl) of sample or control genomic DNA (gDNA). 50 µl of mineral oil was layered on top to prevent evaporation. PCR was performed on the Biometra UNO-thermoblock PCR thermocycler using the following programme. An initial cycle of a denaturing step of 94°C 3 minutes, annealing step 58°C 1minute and an extension step of 72°C 2 minutes followed by 35 core cycles of 93°C 40 seconds, 58°C 1 minute, 72°C 30 seconds and a final cycle of 93°C 40 seconds, 58°C 1 minute and 72°C 3 minutes. Electrophoresis was performed on the samples through a 2.5% agarose gel (Gibco) containing 0.5µg.ml^{-1}ethidiumbromide. The gel was both prepared with and run in Tris acetate ethylene-diamine-tetra-acetate buffer (TAE-see appendix). Samples were prepared with bromophenyl blue loading dye (see appendix) In each case positive and negative controls were included in the gel run as was sterile water to check for contaminating nucleic acids. Gels were viewed on a Herolab UVT-28M transilluminator to reveal bands and images captured with the COHU CCD camera system attached to a Sony Digital Image printer. Figure 2.

2.1.2.3 PCR amplification to identify rumpshaker gene mutation

To each "ready to go PCR bead" (Amersham Bioscience) was added 24µl of prepared master-mix (0.5µl primer α-intron 3, (sequence C (5-CATCACCTATGCCCTGA-3)) 0.5µl primer α-intron 4, (sequence D(5-TACATTCTGGCATCAGCGCCAGAGACTGC-3)) (Schneider et al., 1992) 23 µl filter sterilized water) and 1µl (25µg/µl) of sample or control gDNA. 50µl of mineral oil was layered over each sample to prevent evaporation of the sample during the PCR run. The following program was performed on the Biometra UNO-thermoblock. An initial denaturing cycle of 94°C for 3mins, 1min annealing at 55°C, and 4min extension at 72°C followed by 35 core cycles of 40secs 93°C, 1 min at 55°C, 2 mins at 72°C, and a final cycle of 40secs at 93°C, 1min at 55°C, and 5mins at 72°C.

Following PCR the DNA was purified using PCR purification kit (Qiagen) eluting in a final volume of 30µl.

The presence of the *rumpshaker* mutation introduces an *Acc*I restriction enzyme site into the cDNA. We digested 10µl of DNA with 1 µl (10u/µl) *Acc*I restriction enzyme (Invitrogen), 1.5µl 10x buffer in a final volume of 15µl at 37° C for 3 hours prior to electrophoresis through a 2.5% agarose gel (Gibco) containing 0.5µg.ml^{-1} ethidium bromide. The gel was both prepared with and run in Tris acetate ethylene-diamine-tetra-acetate buffer (TAE). In all cases positive and negative controls were included in the gel run, as was sterile water to check for contaminating nucleic acids and samples were prepared with Bromophenyl blue loading dye. Figure 3.

2.2 Tissue fixation and preparation

2.2.1 Karnovsky's modified fixative

This fixative (Griffiths et al., 1981) was used for the preservation of tissues prepared for resin embedding for light and electron microscopy. Fixed tissues were stored at 4°C until processed. (see appendix).

2.2.2 4% Paraformaldehyde

4% paraformaldehyde prepared in phosphate buffered saline (PBS) was used for the fixation of tissues intended for cryopreservation and subsequent immunohistochemistry. Following perfusion and dissection tissues were immersed in fixative for 3-6 hours before transferring to 20% sucrose in PBS for 24 hours prior to rapid freezing

2.2.3 Perfusion

Mice were humanely euthanased using an overdose of carbon dioxide in a closed chamber. The carcass was pinned out the chest opened and the pericardium removed, to allow cardiac perfusion the right atrium was punctured to allow drainage and a needle was inserted into the left ventricle. Saline was injected under moderate pressure to flush the vasculature. Once the effluent was clear, between 50 ml and 100 ml of fixative was flushed through. Following perfusion the animal was immersed in fixative for up to 3 hours prior to dissection. The brain, optic nerves and spinal cord were removed, cut into appropriate blocks, placed in fixative and stored until further processing.

2.2.4 Resin processing and sectioning

Tissue blocks prepared for resin embedding were processed using a Lynx el microscopy tissue processor (Leica). The tissues were passed through increasingly graded alcohols (see appendix) and infiltrated with araldite resin. The tissue blocks were oriented in resin-filled silicone moulds and placed at 60°C for 24 hours to allow polymerisation. Utilising an Ultracut-E ultratome (Reichert-Jung), 1µm sections, for examination by light microscopy, were cut with a glass knife and the sections mounted on cleaned glass microscope slides, whilst for electron microscopic study, 70nm sections were cut with a diamond knife and mounted on 200-mesh 3.05mm-diameter copper grids.

2.2.5 Cryopreservation and sectioning

Tissue blocks from fresh and 4% paraformaldehyde or P-L-P perfusion fixed animals were suspended in Tissue-Tec O.C.T compound (Miles Inc) filled foil moulds and frozen in isopentane cooled in liquid nitrogen. The frozen blocks were wrapped with NescoFilm (Bando Chemical Ind. Ltd.) and stored at -20°C until required. 15µm sections were cut using an OTF cryostat (Bright Instrument Company) and mounted onto APES-coated microscope slides (see appendix) that were then stored at -20°C.

2.3 Staining techniques and Immunohistochemistry

2.3.1 Methylene blue/ azur II

1µm resin sections were dried onto microscope slides on a 60°C hot plate. The sections were flooded with methylene blue/azurII (see appendix) stain for 30-60 sec and rinsed in running water. After drying, slides were mounted in DPX.

2.3.2 Electron microscopy (EM)

For electron microscopy, the 70nm resin sections on copper grids were “stained” with uranyl acetate and lead citrate (see appendix) examined and images captured on the JEOL CX100 electron microscope.

2.3.3 ABC Technique (Avidin biotin complex)

This technique was utilised for immunolabelling resin sections with anti-MBP in order to facilitate the measurement of myelin density. To enable staining, the araldite resin was etched from the sections by agitation of the slides in sodium ethoxide (50% ripened saturated sodium ethoxide 50% absolute alcohol) for 30 minutes. Slides were washed in absolute alcohol (6 changes) over 30 minutes. Endogenous peroxidase activity was quenched using 3% hydrogen peroxide in water for 30 minutes. Sections were again washed in running water for 30 minutes. Non-specific immunoglobulins were blocked with 10% normal goat serum (NGS) in PBS for 2 hours at room temperature. Excess NGS was removed and primary antibody, diluted in 1% NGS/PBS, was immediately applied and the sections incubated overnight in a humidity chamber at 4°C. Sections were allowed to warm to room temperature and washed in several changes of PBS. Biotinylated anti rat link antibody diluted in 1% NGS was applied for 1 hour at room temperature and then washed in PBS 6 changes over 30 minutes. Sections were incubated with ABC complex (Vectastain elite) for 30 minutes at room temperature and again washed in PBS, 6 changes. The chromogen was developed in filtered PBS containing 0.5 $mg.ml^{-1}$ 3,4,3,4-tetraminobipheyl hydrochloride (DAB) and 0.003% hydrogen peroxide for up to 5 minutes. Excess DAB was removed by washing in PBS for 2 minutes and running water for 5 minutes. The chromogen was intensified with 1% osmium tetroxide. The slides were then dehydrated in alcohols, cleared in xylene and mounted in DPX.

2.3.4 Immunofluorescence

Indirect immunofluorescence was the preferred method of labelling frozen cryostat sections. The sections were allowed to come to room temperature before washing in PBS to remove the Tissue-Tec. If the tissue had not been perfusion fixed then the sections were immersed in 4% paraformaldehyde for 20 minutes and washed once in PBS. Some antibody labelling required permeabilisation in -20ºC methanol or 0.5% triton X-100 (Sigma), others required non-specific immunoglobulins to be blocked with 10% Normal goat serum (NGS) or 0.1% tritonX-100 with 0.2% pigskin gelatin (Sigma). Primary antibodies were diluted in 1% NGS or triton/gelatin blocking buffer, as above, the sections were incubated in primary antibody overnight at 4ºC. On day 2, sections were allowed to come to room temperature before being washed in several changes of PBS. Secondary antibodies labelled with fluorescein isothiocyanate (FITC) or Texas red (TxR) were diluted in PBS or the blocking buffer as before and applied to the sections for 30 minutes at room

temperature. Slides were briefly washed in PBS before mounting in antifade mounting medium (Citifluor). Sections were examined by epifluorescence. FITC absorbs light with a wavelength 495 nm and emits it at 525 nm, which can be visualised as green light using a blue filter. TxR absorbs light at 596 nm and emits it at 620 nm, which can be visualised as red light using a green filter. 4,6-diamidino-2-phenylindole (DAPI), a nuclear marker employed, provides a blue fluorescent light with excitation of 345 nm and emission of 455.

2.3.5 Antibodies and Markers

Commercially available and gifted antibodies were used and their sources and dilutions are illustrated in Table 1. Anti-Caspase-3 antibody was used to recognise apoptotic cells. APC (Adenomatous Polyposis Coli) has an affinity for CC-1 and was employed to distinguish mature oligodendrocytes (Fernandez et al., 2000; McTigue et al., 2001). Anti-CD45 antibody recognises pan-leukocytes and was used to identify microglia/macrophages. Anti-MBP antibody was used to stain central compact myelin.

Table 1

Antibody	Isotype	Dilution	Source
Caspase 3	Rabbit	1:4000	R&D
CC-1 (APC)	IgG2b	1:100	Calbiochem
MBP	Rat	1:500	N.P Groome (Gift)
CD45	Rat	1:600	Serotec

Table 2

Secondary Antibody	Dilution	Source
Rabbit FITC	1:80	Southern Biotech
Rat FITC	1:50	Southern Biotech
MouseIgG2b	1:100	Southern Biotech

CC-1 staining of oligodendrocytes

15µm cryostat sections from 4% paraformaldehyde perfused blocks were permeabilised in 0.5% triton X-100 for 30 minutes and non-specific binding blocked with 0.1% triton X-100, 0.2% pigskin gelatin in PBS for 30 minutes. Excess blocking solution was removed and CC-1 antibody at 1:100 diluted in blocking solution applied and the sections incubated at 4°C overnight. The slides were washed in PBS and incubated with goat anti-mouse IgG2b FITC secondary antibody diluted in blocking solution for 30 minutes, the nuclei stained with DAPI and the slides washed and mounted. CC-1 has been used to label mature oligodendrocytes (McTigue et al., 2001).

CD45 staining of microglia

Animals were perfusion fixed with periodate-lysine-paraforfaldehyde fixative (P-L-P see appendix) Sections were permeabilised in methanol at –20°C for 10 minutes and washed in PBS. The sections were incubated with anti-CD45 in 1% NGS at 4°C overnight. Following PBS wash, goat anti-rat IgG FITC secondary antibody was applied to the sections at room temperature for 30 minutes, rinsed in PBS and counterstained with DAPI before mounting

Caspase-3 staining of apoptotic cells

Following permeabilisation in 0.5% triton X-100 sections were blocked with 0.1% triton X-100, 0.2% pigskin gelatin in PBS for 30 minutes. Excess blocking solution was removed and anti-caspase-3 antibody diluted in blocking solution was applied and the sections incubated at 4°C overnight. The sections were washed and incubated with goat anti-rabbit IgG FITC secondary antibody diluted in blocking solution for 30 minutes the nuclei stained with DAPI and the slides washed and mounted.

DAPI Staining

Following immunolabelling cell nuclei were stained with 0.83µg.lml-1 4,6-diamidino-2-phenylindole (DAPI), the fluorescent dye, for 30-60 seconds.

2.4 Quantitative studies and statistical analyses

2.4.1 Myelin volume

Cervical segment 2 (C2) of spinal cord was dissected following perfusion-fixation in Karnovsky's Modified Fixative and processed for resin embedding. Following polymerisation the resin blocks were trimmed and thin sections (70nm) cut from the ventral columns of the white matter tract and placed onto copper grids, which were subsequently stained with uranyl acetate and lead citrate.

Using the Jeol CX-100 Electron microscope set at a magnification of x4000, ten micrographs from each sample were randomly selected and printed at ~3.5x enlargement to occupy an A4 sheet of printing paper. The myelin volume of each genotype was derived using a point counting technique (Williams, 1977). A grid pattern ($2cm^2$) was superimposed over each print and the number of gridline intercepts overlying areas of compact myelin expressed as a ratio of the total number of gridline intercepts.

Vv = Points overlying compact myelin/Total points available on grid.

2.4.2 Axon status

Utilising the same photomicrographs as above a simple line grid (2 lines running diagonally from corner to corner) was overlayed and the number of non-myelinated and myelinated axons touching the line were counted. The number of each was expressed as a percentage of total number of fibres.

2.4.3 g ratio

Axon and total fibre diameters were measured with Image ProPlus-4 software (Media Cybernatics, Silver SpringMD) from digital images of the ventral columns of 0.5µm resin sections taken with x100 oil immersion lens. From these data the myelin thickness and g ratio (ratio of axon diameter to total fibre diameter) were calculated.

2.4.4 Myelin Density

Myelin area was measured on semi thin (1µm) resin sections immunolabelled with anti Myelin Basic Protein using the ABC technique. Four areas, two either side of the ventromedian fissure were captured (x40 dry lens) using a CCD camera (Colour Coolview, Photonic Science). The digital images were converted to grey scale using Image Pro Plus software (Media Cybernetics). An area of interest (AOI) of 2500µm^2 was placed over two separate areas of each of the four captured images and the total area of black objects (MBP labelled myelin) measured. The density of myelin (µm^2/mm^2) of white matter was calculated.

2.4.5 Quantification of CC-1+ cells

Cell counts were performed on the ventral columns of cryosections (15µm), adjacent to the ventromedian fissure, from rostral cervical spinal cord. Images of CC-1-labelled cells (green channel) and DAPI-labelled nuclei (blue channel) from the same sampling area were collected (x20) using a CCD camera system (Photonic Science Colour Coolview) and stored in the computer. The green and blue channels were merged using Adobe Photoshop (Adobe systems Inc., San Jose) and the image quality adjusted. For each combined image, a frame (35804µm2) outlining the AOI was placed on the screen. The number of APC+ cell bodies containing a DAPI-stained nucleus was counted within the AOI or touching the top or left side but excluding those touching the bottom or right sides. The density of DAPI-labelled nuclei was counted automatically with an AOI of 10,000µm^2. The density

of CC-1-labelled cells with DAPI-stained nuclei (nuclei/mm^2) was calculated and the percentage of CC-1+ve cells (CC-1 cells/DAPI nuclei x 100) calculated.

2.4.6 Quantification of CD45+ cells and caspase3+ cells

These cells were quantified as described for the CC-1+ cells (2.4.5).

2.4.7 Calculation of cell numbers

Quantification of cells or nuclei was determined by density in the ventral funiculi. As the area of the white matter varied between different genotypes we calculated the total number of cells/nuclei in the white matter of a transverse section. This calculation assumes that the density is equally distributed throughout the white matter when there is actually variation between tracts and at different ages. In fact the nuclear density alters across the width of the ventral column, being greater in the central region adjacent to the grey matter. The alternative strategy is to define a precise sub-region of the ventral column in which to calculate total numbers, a task that would be problematic in ensuring consistent identification of the chosen region. The calculation based on the total white matter area therefore offers an acceptable way of comparing cell numbers between different genotypes and ages.

2.4.8 Statistical analysis

Group sizes

The number of animals included in a group varied between ages, genotype and techniques. In general, 4 or more animals were included in a group.

Data presentation

Graphs are presented as mean ± SEM. P values are denoted as $*$ <0.05, $**$ <0.01, $***$ <0.001.

Statistical tests

As group sizes were always relatively small no assumptions were made that the data was distributed normally. Groups were first compared using one-way Analysis Of VAriation (ANOVA). If a significant difference ($p<0.05$) was detected, individual groups were compared using the Bonferroni multiple comparison test. Comparison of only the two mutant groups used the grouped t test. Analyses were performed using GraphPad prism 4 (GraphPad software Inc, San Diego CA.)

2.5 Biochemical Analysis

2.5.1 Myelin fraction preparation

This technique was used to extract myelin from CNS tissue and is based on the method of Norton and Poduslo (1973a). The principle is based on centrifugal enhanced flotation of the myelin fraction due to the highly buoyant nature of lipids. By-products of the technique include the pellet fraction containing the membranous and nuclear components of the spinal cord and the supernatant representing the cytoplasmic components.

Spinal cords snap frozen in liquid nitrogen and stored at -70ºC, from freshly euthanased animals were used in the preparation of the fractions.

Initially the cord was thawed in 7.5ml high sucrose buffer (0.85M sucrose, 10mM Hepes, 2mM Dithiothreitol, 1mM TLCK) and homogenised using an IKA ultra turrax polytron homogeniser at high speed for 12-15 strokes. 500µl of the resultant homogenate was retained and represents the total homogenate, the remainder was transferred to a Beckman centrifuge tube and 3ml of low sucrose buffer (0.25M sucrose, 10Mm Hepes) gently layered on top. The samples were centrifuged at 70000g, 90minutes, 4ºC using SW41 rotor on a Beckman ultracentrifuge. Following centrifugation the myelin fraction could be clearly visualised at the interface of the two sucrose solutions. The upper layer was aspirated and the myelin interface collected to a fresh tube, 6mls of chilled milliQ water (Millipore System) was added to each sample causing osmotic shock. The samples were vortexed and centrifuged at 23000g, J21 rotor, 4ºC, 30 minutes. The supernatant was removed and the process repeated a further 2 times with the exception that the third spin was performed at 17000g, this ensures that the myelin is as “clean” as possible. The final pellet was resuspended in a volume of milliQ water dependant on the size of the pellet, the

intention being to have each sample at a similar concentration. From a representative sample group the *rumpshaker* myelin pellet, being the smallest of the samples, was resuspended in 75µl, the transgene-complemented *rumpshaker* pellet resuspended in 150µl and the wild type pellets in 600µl. Aliquots of fractions generated from the initial high speed 70000g spin were collected for subsequent analysis, 1ml of the sucrose supernatant, enriched in the soluble cytoplasmic fraction and the pellet fraction enriched in membranous and nuclear elements resuspended in 2ml 0.25M sucrose. All fractions were stored at -20ºC.

2.5.2 Oligodendrocyte culture preparation

Oligodendrocytes were prepared from the spinal cord of postnatal day 5 animals by the method described (Fanarraga et al., 1995). Animals were euthanased in a halothane chamber and decapitated to ensure exsanguination. Using sterile technique and with the aid of a dissecting microscope the spinal columns were removed and the cord dissected out into Hanks balanced salt solution without calcium or magnesium (Invitrogen) the meninges were stripped from the cord and the cord masticated with a sterile scalpel. The connective tissue of the cord was digested by the addition of 1ml 0.25% trypsin (Invitrogen) and 100µl 1% collagenase type 1(MP Biomedicals) and incubation at 37ºC for 30minutes, followed by a second dose of trypsin/collagenase and incubation for 30 minutes. The digestion was quenched by the addition of 1ml Stop solution (see appendix). The cord triturated through 23g needle (3 times) and 26g needle (3 times) before the addition of DMEM 10% (see appendix), and centrifugation at 800rpm 5minutes. The supernatant was removed and the pellet resuspended in 1ml DMEM/10%. The cell suspension was plated onto 2x 35mm poly-D-Lysine treated tissue culture dishes (see appendix) and the cells allowed to settle down onto the plate for 2hours in a LEEC tissue culture incubator at 37ºC with 5% CO_2 before the addition of 1.5ml Sato conditioned medium (see appendix) The cultures were incubated for 7days in the incubator before harvesting. Although the cultures were a mixed population of cells the conditioned growth medium employed favoured oligodendrocyte proliferation.

Cell Lysis

Tissue culture plates were removed from the incubator and immediately washed with chilled PBS. 75µl of cell lysis buffer (see appendix) was added to each plate incubated on ice for several minutes and the adherent cells removed from the surface of the plate utilising a cell scraper. The cell suspension was then transferred to a tube and rotated end

over end at 4˚C for 30 minutes. The debris was precipitated by centrifugation at 5000rpm at 4˚C for 5minutes and the cell lysate transferred to a fresh tube and stored at -20˚C until required.

2.5.3 Protein Assay

Protein concentrations were quantified in order to ensure equal loading of samples on subsequent gels. The assay was performed using the Pierce protein assay system (Perbio) based on the Lowry Method using bicinchoninic acid (BCA) as the reagent. The reaction was initiated by the addition of the reagent and incubated at 37ºC for 30 minutes. 2mg/ml BSA standards (precision plus all blue protein, Biorad) were diluted (0.025, 0.05, 0.1, 0.2, 0.4, 0.6mg/ml) and prepared at 10X the concentration of the samples, which were routinely 5µl of sample/1ml of reaction reagent. Measurement of the absorbance of the final product was performed on a spectrophotometer (Cecil 1100) set to a wavelength of 562nM. A standard curve was generated and the sample concentrations calculated from this.

2.5.4 SDS PAGE (sodium dodecyl(lauryl)sulphate polyacrylamide gel electrophoresis)Western Blot

At the onset of the project gels were hand poured from stock solutions (table 4) Laterly precast gels were employed for safety, convenience, economy of time and reproducability. Precast gels employed were Novex Nupage 4-12%, 10 or 12 well (Invitrogen) with MES page buffer (Invitrogen)

Gel preparation

The gel tank system used for precast gels was the Invitrogen Mini gel system, although these gels were also compatible with the Atto system (Atto Corporation) employed for the hand poured gels. Various combs were used depending on the number of samples to be run.

Sample Preparation

The samples were prepared to a total volume of 24µl including 8µl of 3x SDS/DTT denaturing buffer (see appendix) and heated to 85ºC for 4 minutes, to linearise the protein and allow SDS association at a uniform charge to protein ratio, prior to running in SDS

PAGE (see appendix) or MES (Invitrogen) running buffer at Standard limits of 250V 200mA and 25W with a constant voltage of 100-150V for approximately 1.5 hours.

Transfer

Following a brief wash in water the gel was removed from the plate and placed in cathode buffer (see appendix) The proteins were transferred to PVDF membrane (Millipore Immobilon-P transfer membrane) using a semi dry blotter and Towbin transfer buffering solutions (see appendix) which enables the transfer. The transfer was carried out at standard limits of 50v 250 mA 15W constant current 225 mA for 1hour. To check the transfer was successful and to check for equal loading, the blot was stained briefly with Ponceau S (see appendix) a water-soluble stain that highlights the proteins.

Immunodetection of protein

Non-specific immunoreactive proteins and peptides were blocked with 5% skimmed milk (Marvel) in Tris buffered saline/tween (T-TBS see appendix) for 2 hours at room temperature or 4ºC overnight before immunolabelling for the specific protein of choice. All primary antibodies (for source and dilutions see table 3) were prepared in 5% skimmed milk/T-TBS and the blots incubated overnight at 4ºC on an ELMI skyline orbital shaker. After washing several times in T-TBS over 30 minutes secondary antibody linked to horseradish peroxidase was applied at a dilution of 1:10,000 (Sigma), again diluted with 5% skimmed milk/T-TBS, 1hour room temperature followed by several washes. The blot was developed with ECL (Super signal West Pico chemiluminescent substrate. Pierce) wrapped in saranwrap and exposed to x-ray film (AGFA) over a range of incubation periods ranging from 30seconds to several minutes to identify the optimal exposure.

Table 3

Antibody	Dilution	Source	Secondary
CNP	1:2000	P Brophy (Gift)	Anti rabbit HRP
MBP	1:5000	Chemicon	Anti rabbit HRP
PLP	1:100,000	In house	Anti rabbit HRP
ASPA	1:1000	J Garbern (Gift)	Anti rabbit HRP
MAG248	1:1000	Chemicon	Anti rabbit HRP
Sirtuin 2	1:500	Cell Signalling	Anti rabbit HRP
Bip	1:2000	Stressgen	Anti rabbit HRP
GFAP	1:200,000	Sigma	Anti rabbit HRP

Quantification of blots

The blots were scanned with an Epson Perfection 4990 Photo scanner to create digital images. Scion Image software (NIH) was used to quantify individual protein bands from the blots. The software generates a graphic output of the pixel density of the selected band and the integral calculated to give signal density.

Statistical Analyses

Analysis was performed using Graphpad Prism 4 software (GraphPad software Inc, San Diego CA). Statistical tests applied were ANOVA and Bonferroni's multiple comparison test and t-test as described previously.

2.6 Molecular Biology

2.6.1 RNA Preparation

Total RNA (tRNA) was extracted from spinal cord samples snap frozen in liquid nitrogen and stored at -80ºC. To minimise potential RN*ase* contamination and subsequent degradation of RNA, work surfaces mortar and pestle etc were sprayed with RnaZAP(Ambion). The RNA was extracted using the RNAsol Bee commercial kit (Tel-test Inc, Friendswood TX), which is based on the Phenol/Chloroform extraction of RNA and separation of nucleic acids from protein due to their differential solubility in protein and non-protein solvents. Spinal cord was ground in liquid nitrogen using mortar and pestle, to generate a homogenous powder, transferred to a 7ml specimen bottle on ice before the addition of 1ml of prechilled RNAsol Bee (homogenous powder assists in rapid inactivation of RN*ase*) The tissue was triturated through hypodermic needles of decreasing gauge (23G, 26G, 30G) several times each. The entire sample was transferred to a 1.5ml microtube 200µl chloroform added and vortexed 20-30 seconds, chilled on ice for 5 minutes and removed from the Phenol/chloroform fraction and 4µl of glycogen added to enable visualization of the RNA before the addition of 500µl of 100% isopropanol. The sample was incubated at room temperature for 10 minutes before centrifugation 13K for 15 minutes 4ºC. The supernatant was poured off and 1ml of 70% filter sterilized ethanol added the sample vortexed and centrifuged 13K, 8 minutes 4ºC and the supernatant aspirated with a pipette to ensure that the excess ethanol was removed. The sample was air dried for 10 minutes and the pellet resuspended in 150µl of DEPC treated water.

The integrity of the RNA was confirmed by gel electrophoresis on a 2% agarose gel containing 0.5ng/ml ethidium bromide; each sample contained Orange G loading dye. Both mRNA and rRNA are visible as sharp bands indicating no decay of the mRNA; there should be no contaminating gDNA band present. The optical density of the RNA was measured with a spectrophotometer to check for salt, solvent or protein contamination and to quantify the RNA yield. The prepared RNA was used in real time quantitative PCR studies (qPCR) and reverse transcriptase-PCR (RT-PCR) studies of *Xbp-1, Chop* and *ATF3.*

2.6.2 Real time quantitative PCR (qPCR)

The ABI prism7500 sequence detection system (Applied Biosystems, Foster City, CA) using TaqMan technologies (PE Biosystems, Foster City CA) was employed following manufacturers instructions. Real time quantitative PCR was performed using the Platinum quantitative RT-PCR Thermoscript one step system (Invitrogen). The PCR primer and probe sets were designed using the program primer-Express™ (Applied Biosystems) The following primer and probe sets were used. *β-actin* (Accession #NM_007393) forward 5′-AGAGGGAAATCGTGCGTGACAT-3′: reverse 5′-AGGAAGGCTGGAAAACAGCC-3′: TaqMan probe 5′-TGGCCACTGCCGCATCCTCTTC-3′. A combined primer probe that amplified both *Plp* and *Dm20* (*Plp/Dm20*) was utilised, forward 5′-GTATAGGCAGTCTCTGCGCTGT-3′: reverse 5′-AAGTGGCAGCAATCATGAAGG-3′: TaqMan probe 5′-TGGCAAGGTTTGTGGCTCCAACCTT-3′. A combined primer set that amplified all *MBP* isoforms(Accession #NM_ 010777) was also utilised 5′-AGACCCTCACAGCGATCCAA-3′: reverse 5′-CCCCTGTCACCGCTAAAGAAG-3′: TaqMan probe 5′-CAAGTACCATGGACCATGCCAGGC-3′. Each probe had FAM at the 5′end and Blackhole Quencher at the 3′end (MWG Biotech, Germany). A standard curve generated from each set using serial dilutions of the RNA prepared from the samples confirmed the linearity of the method. The samples were run with the following program, 30mins at 50ºC, 10mins at 95ºC followed by 40 cycles of 15secs at 94ºC and a final 2mins at 64ºC. Analysis was carried out by relative quantification using Ct values of the *Plp/Dm20, Plp* and *MBP* probes versus *β-actin*. Normalised expression of target message probe with respect to *β-actin* message was determined for all samples to generate mRNA per 50µg total RNA initially loaded. The relative amounts of transgene-complemented *rumpshaker* and *rumpshaker* mRNAs were expressed as a percentage of wild type.

2.6.3 RT-PCR for XBP-1, Chop and ATF3

RT-PCR was performed on the sample mRNA (prepared as described 2.6.1) using primers (MWG, Germany) for XBP-1, forward 5′-AAACAGAGTAGCTCAGACTGC-3′ and reverse 5′-TCCTTCTGGGTAGACCTCTGGGAG-3′. The PCR products were then digested with *Pst 1* (Invitrogen), which cuts only the unspliced cDNA. The spliced and unspliced products were resolved on a 2.5% agarose gel (Invitrogen) containing ethidium bromide. Control samples of RNA from oligodendrocyte cultures exposed to DTT, to stress the cells, were processed simultaneously. Primers for *Chop* (MWG) were forward 5′-CATACACCACCACACCTGAAAG-3′, and reverse

5′-CCGTTTCCTAGTTCTTCCTTGC-3′ (accession# X67083.1) a product size of 356bp, and those for *ATF3* (MWG) forward 5′-CAACATCCAGGCCAGGTCT-3′, and reverse 5′-CTCTGCAATGTTCCTTCTTTT-3′, (accession# BC064799.1) a product size of 532bp. Cyclophilin was used as an internal control for invariant gene expression when analysing these two products which were resolved on a 2% agarose gel with ethidium bromide, a 1Kb ladder (Invitrogen) was included on each gel and the samples were loaded with Bromophenol blue loading dye. The captured images were quantified using the Scion image software correcting the intensity of the signals for the density of the cyclophilin.

Lane # **1 2 3 4 5 6 7 8 9**

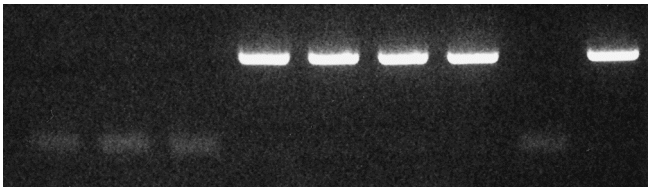

Figure 2. PCR products run on agarose gel. PCR performed using primers to reveal presence of #66 transgene. Lanes 1-3 transgene negative samples, lanes 4-7 transgene positive samples, lane 8 negative control and lane 9 positive control.

Lane # **1 2 3 4 5 6 7 8 9**

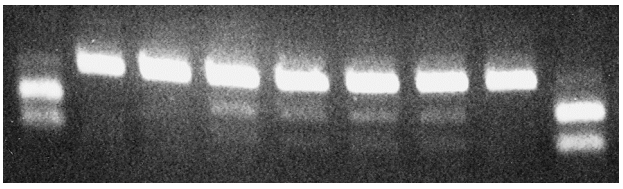

Figure 3. Acc1 digested PCR products run on agarose gel performed to reveal *rumpshaker*, transgene-complemented *rumpshaker* and wild type genotypes. Lane 1 *rumpshaker,* lane 2-3 wild type, lane 4-7 transgene-complemented *rumpshaker*, lane 8 wild type control, lane 9 *rumpshaker* control.

3. Comparison of clinical and pathological phenotype in *rumpshaker, Plp1* transgene complemented *rumpshaker* and wild type mice.

3.1 Survival study

3.1.1 Introduction

Rumpshaker mice on the C57BL/6 background present clinically with severe tremor from the second week of life and go on to develop seizures during the fourth week of life with the majority of animals dying in the fifth or sixth week (Al-Saktawi et al., 2003). I evaluated the survival time of these animals and others complemented with the *Plp1* transgene for up to 40 days.

3.1.2 Method

The offspring from a female C57BL/6 *rumpshaker* heterozygote and a C57BL/6 wild type male carrying the #66 *Plp1* transgene were allowed to survive for up to 40 days postnatally, the longest time period approved by the Home Office. A tail tip was collected from any animal that died prematurely to allow the genotype to be ascertained.

3.1.3 Results

Fewer seizures were observed in the transgene-complemented *rumpshaker* mice and all survived up to 40days. Survival curves indicate a median survival of 35 days in the unmodified *rumpshaker* mice, significantly different from the transgene-complemented *rumpshaker* mice. The wild type mice also survived to P40, identical to the transgene-complemented *rumpshaker* mice. (Figure 4.)

3.2 Quantification of Myelin

3.2.1 Introduction

Within the normal CNS the majority of axons are myelinated. Dysmyelination is a common feature of animals carrying a mutation of the *Plp1* gene. As described previously (1.4.2), myelin is a highly organised multilamellar structure composed of 70% lipid and 30% protein. I studied the effect on the *rumpshaker* phenotype of introducing a wild type *Plp1* transgene. Peak myelination occurs around postnatal day 20 (P20), therefore, the bulk of my study focussed on that age point.

3.2.2 Materials and methods

3.2.2.1 Myelin density

Myelin density was quantified using 1µm sections of P20 and P40 cervical spinal cord immunostained for myelin basic protein (MBP) as described previously (2.4.4). The amount of myelin positively stained is expressed as area of MBP staining per $mm^{2.}$

3.2.2.2 Myelin volume

Since MBP immunostaining can label uncompacted myelin, the volume of compact myelin was quantified using electron micrographs of the ventral columns of C2 spinal cord at P20 and a point counting method as described (2.4.1).

3.2.2.3 Percentage of myelinated fibres

Utilising the same micrographs as above the percentage of myelinated axons was quantified (2.4.2).

3.2.2.4 g ratio

0.5 µm resin sections were used to determine g ratio (the ratio of axon diameter to total fibre diameter.

3.2.2.5 Myelin periodicity

High magnification electron micrographs were examined to assess the periodicity of the myelin.

3.2.2.6 Hardware and Software

A colour Coolview camera (Photonic Science) with Image ProPlus 4 software (Media Cybernetics) imaging system was used to assist in the quantification.

3.2.3 Results

3.2.3.1 Myelin density

At both ages the *rumpshaker* and transgene-complemented *rumpshaker* animals had less myelin than the wild type animals; (Figure 5) however, expression of wild type PLP/DM20 in the transgene-complemented *rumpshaker* animals significantly increased the myelin compared to the *rumpshaker* animals. (Figure 6A.)

3.2.3.2 Myelin volume

The transgene-complemented *rumpshaker* animals had significantly more compact myelin than the *rumpshaker*, but both *rumpshaker* and transgene-complemented *rumpshaker* had less than the wild type. (Figure 6B.)

3.2.3.3 Proportion of myelinated axons

The proportion of myelinated axons was significantly increased by the presence of wild type PLP/DM20 in the transgene-complemented *rumpshaker* animals compared with *rumpshaker*. (Figure 7A.)

3.2.3.4 g ratio

The g ratio was significantly increased in both the *rumpshaker* and transgene-complemented *rumpshaker* animals compared with wild type. (Figure 7B.)

3.2.3.5 Myelin periodicity

rumpshaker myelin has reduced periodicity and the intraperiod line (IPL) and major dense line (MDL) are hard to distinguish. The periodicity was recovered by expression of the transgene. (Figure 8D.)

3.3 Quantification of glial cell apoptosis

3.3.1 Introduction

Oligodendrocyte cell death is a prominent feature of *Plp1* missense mutations (Cerghet et al., 2001; Skoff, 1995) Programmed cell death (apoptosis) is characterised by activation of the caspase cascade, including caspase 3, an effector caspase expressed in oligodendrocytes, which is a classic marker of apoptosis (Momoi, 2004). Histopathologically, dead cells are characterised by pyknotic nuclei with condensed chromatin. I used both histopathological identification and immunostaining to quantify the numbers of apoptotic glia. In addition, I quantified the numbers of microglia/macrophages present.

3.3.2 Materials and methods

3.3.2.1 Quantification of pyknotic nuclei

Quantification was performed on 1µm resin sections of cervical spinal cord (C2) stained with methylene blue/azurII (see 2.3.1). Pyknotic nuclei in all white matter tracts were counted.

3.3.2.2 Quantification of Caspase 3 positive cells

15µm cryo sections were immunostained with caspase3 antibody (see 2.3.5). Counts were performed from 4 areas on the ventral columns of the cervical 2 segment of spinal cord at postnatal day 20 and 40 (P20, P40). The immunostained sections were counterstained with a nuclear marker DAPI (see 2.3.5), only caspase 3 positive cells containing a nucleus were counted.

3.3.2.3 Quantification of oligodendrocyte numbers

The numbers of CC-1 positive oligodendrocytes in the ventral columns of cervical 2 spinal cord were counted (see 2.3.5.). In addition, double immunostaining with anti-CC-1/ anti-caspase 3 was performed.

3.3.2.4 Quantification of Macrophages/microglia

The number of macrophages/microglia present in 15µm cervical 2 sections of spinal cord were counted by immunostaining with the pan leucocyte marker CD45.

3.3.3 Results

3.3.3.1 Pyknotic nuclei

At P20 both the *rumpshaker* and transgene-complemented *rumpshaker* mice had elevated numbers of pyknotic nuclei compared to the wild type animals; however, the presence of the transgene significantly reduced the number when compared to *rumpshaker*. At P40, the overall numbers of pyknotic nuclei in all genotypes were reduced; however, the differences between genotypes remained unchanged. (Figure 10A.)

3.3.3.2 Caspase 3 positive cells

The counts of activated caspase 3 positive oligodendrocytes in the ventral columns showed an identical profile to that of the pyknotic nuclei at P20. (Figure 10B.)

3.3.3.3 CC-1 positive cells

The number of CC-1 positive oligodendrocytes was comparable across all three genotypes (Figure 11A.). The number of double stained CC-1 positive/ caspase 3 positive cells was also reduced in the transgene-complemented *rumpshaker* animals compared to *rumpshaker*.

3.3.3.4 CD45 positive cells

The numbers of CD45 positive macrophages/microglia were the same for *rumpshaker* and transgene-complemented *rumpshaker*, each having a fivefold increase from wild type. (Figure 11B.)

3.4 Discussion

Data presented in this chapter show that the transgene-complemented *rumpshaker* animals live longer than the unmodified *rumpshaker* mice. The myelin status in the transgene-complemented *rumpshaker* animals is improved with an increase in the amount of myelin. Additionally, the proportion of myelinated axons is increased and the periodicity of the myelin is returned to that of wild type, conversely, the g-ratio is not significantly improved. The number of apoptotic oligodendrocytes is reduced in the transgene-complemented *rumpshaker* animals; however, there is no change in the number of microglia/macrophages, which remain elevated compared to wild type.

The presence of wild type PLP has a marked effect on the survival of the animals. In this study I examined and quantified the most common characteristics of myelin mutants, dysmyelination and apoptosis of oligodendrocytes, to try to identify the key parameters that would account for the improved survival. Although the amount of myelin is increased in the transgene-complemented *rumpshaker* animals, the level is still significantly reduced compared to that of wild type animals. Since the g ratio is not significantly improved, the increase must be attributed to the greater number of myelinated axons. McLaughlin (McLaughlin et al., 2006) demonstrated that misfolded *rumpshaker* PLP is inserted into the myelin sheath. In transgene-complemented *rumpshaker* myelin it is possible that the majority of the misfolded *rumpshaker* PLP is replaced by wild type PLP, which returns the periodicity to normal.

It is true that mice with hypomyelination die prematurely and that severe hypomyelination causes earlier death, studies by Billings-Gagliardi (Billings-Gagliardi et al., 1999) and Wolf (Wolf et al., 1999) revealed that contrary to the accepted view, hypomyelination is not the cause of premature death. There is also a relationship between hypomyelination and severity of apoptosis in *Plp1* myelin mutants, decreasing amounts of myelin corresponding with increased apoptosis, determining the relationship between the two is complicated. Skoff (Skoff et al., 2004) has proposed that apoptosis of oligodendrocytes occurs initially and that hypomyelination follows as a result of the reduced numbers of oligodendrocytes. They show that inhibiting the synthesis of mutant PLP reduces apoptosis and that the subsequent increase in myelin can be attributed to more oligodendrocytes surviving rather than a proliferation of new oligodendrocytes. However Al-Saktawi (Al-Saktawi et al., 2003) found no difference in the number of oligodendrocytes in C57 *rumpshaker* when compared with wild type, the number of apoptotic oligodendrocytes in *rumpshaker* being

matched by the number of proliferating oligodendrocytes. Indeed in my study the CC-1 immunostaining indicated comparable numbers of oligodendrocytes in each of the three genotypes. Furthermore, Thomson (Thomson et al., 1999) showed that in the first week of life oligodendrocyte numbers in *jimpy* mice were similar to wild type mice but that the amount of myelin was only 20% of wild type and that only a minority of axons were ensheathed by myelin, suggesting that myelin mutant oligodendrocytes are unable to properly associate with axons resulting in hypomyelination and that the subsequent apoptosis can be attributed to a lack of trophic support to the oligodendrocytes which fail to connect with an axon. We cannot distinguishing *rumpshaker* PLP from wild type PLP, therefore cannot determine if transgene-complemented *rumpshaker* oligodendrocytes are synthesising wild type PLP capable of associating with axons, and that the increase in myelin is a direct result of this. We could utilise a genetic approach and breed a caspase-3 deficient mouse with our *rumpshaker* mouse to produce a cross in which apoptosis of oligodendrocytes would be reduced. If there was an improvement in survival it would suggest that apoptosis is the primary cause of hypomyelination and is also related to survival.

Seizure is another well-documented characteristic of myelin mutants and indeed both the C57BL/6 *rumpshaker* and transgene-complemented *rumpshaker* mice manifest this characteristic. A common cause of seizure is hypoxia. Miller (Miller et al., 2003) have reported that the myelin-deficient (*md*) rat develops “lethal hypoxic depression of breathing at postnatal day 21,” the age at which these animals die prematurely. They describe pathological changes in the respiratory control centre located in the caudal brainstem of these animals, including severe dysmyelination and the presence of immunoreactive PLP/DM20 in neurones.

A further notable characteristic of the *rumpshaker* phenotype is the macrophage/microglial response. It is unclear if this is primarily an effect of cell death and tissue damage or if it is part of the causal mechanism. The fact that there is no discernable difference between the *rumpshaker* and the transgene-complemented *rumpshaker* mice may indicate that the inflammatory response is unimportant in determining the severity of the pathology. It would be possible to assay a panel of cytokines in these two genotypes to determine if any change in expression was induced by the transgene. Alternatively, we could treat the animals with minocycline to inhibit microglial activation (He et al., 2001) and determine if there was any improvement in phenotype or survival. A further approach would be to attenuate the macrophage response by crossbreeding sialoadhesin deficient mice (Ip et al., 2006) with our *rumpshaker* mice and again, determine any improvement.

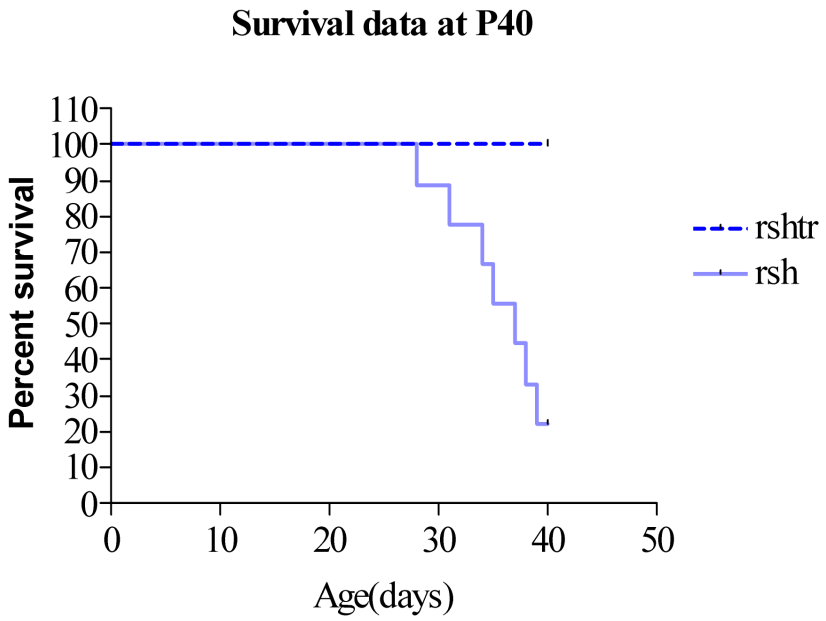

Figure 4. Survival curves from *rumpshaker* (*rsh*) and transgene-complemented *rumpshaker* (*rsh*tr) mice. All transgene-complemented *rumpshaker* survived to postnatal day 40, the oldest age studied.

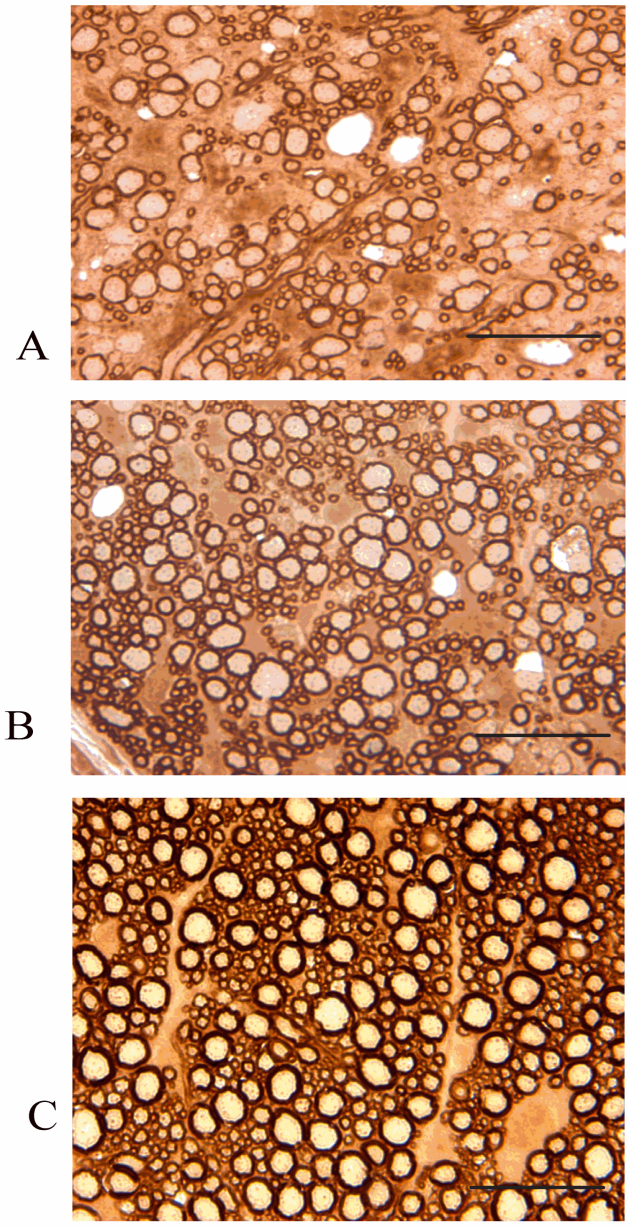

Figure 5. Images from ventral columns of 1µm resin sections immunostained for MBP. **A** - *rumpshaker*, **B**- transgene-complemented *rumpshaker*, **C** -wild type. The image of r*umpshaker* demonstrates that significantly fewer axons are surrounded by sheaths immunolabelled with MBP, an increased in immunolabelling is seen in the image of transgene-complemented *rumpshaker*. Images 100x oil and bars= 20µm.

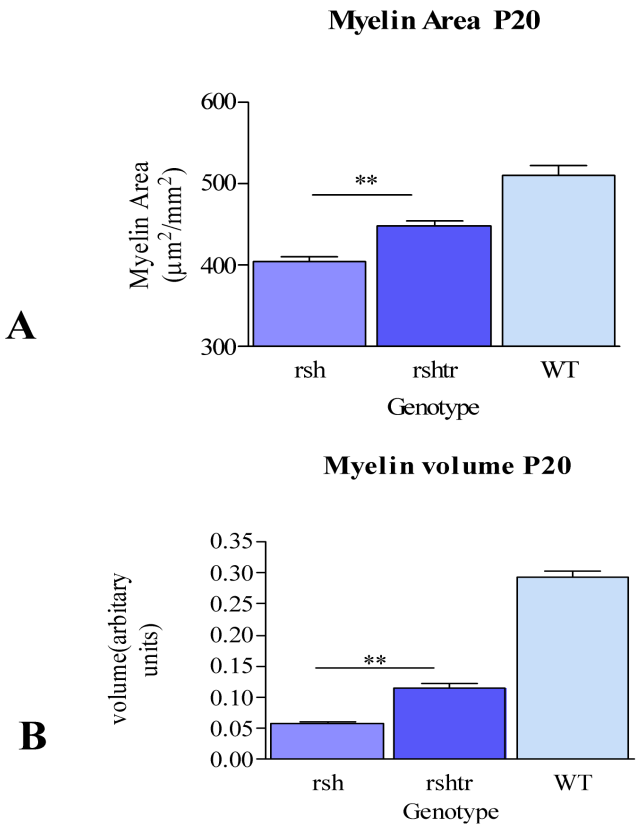

Figure 6A. Graph of myelin density expressed as area of MBP positive immunostaining per mm^2 performed on 1µm resin sections of cervical spinal cord at P20. Both *rumpshaker* (rsh) and transgene-complemented *rumpshaker* (rshtr) are lower than wild type (WT), however *rumpshaker* is significantly reduced compared with transgene-complemented *rumpshaker*.

Figure 6B. Graph of myelin volume. Counts were performed on electron micrographs (x4000) overlaid with a point counting grid. *rumpshaker* (rsh) is significantly reduced compared to transgene-complemented *rumpshaker* (rshtr). Both mutants are well below the wild type (WT) value.

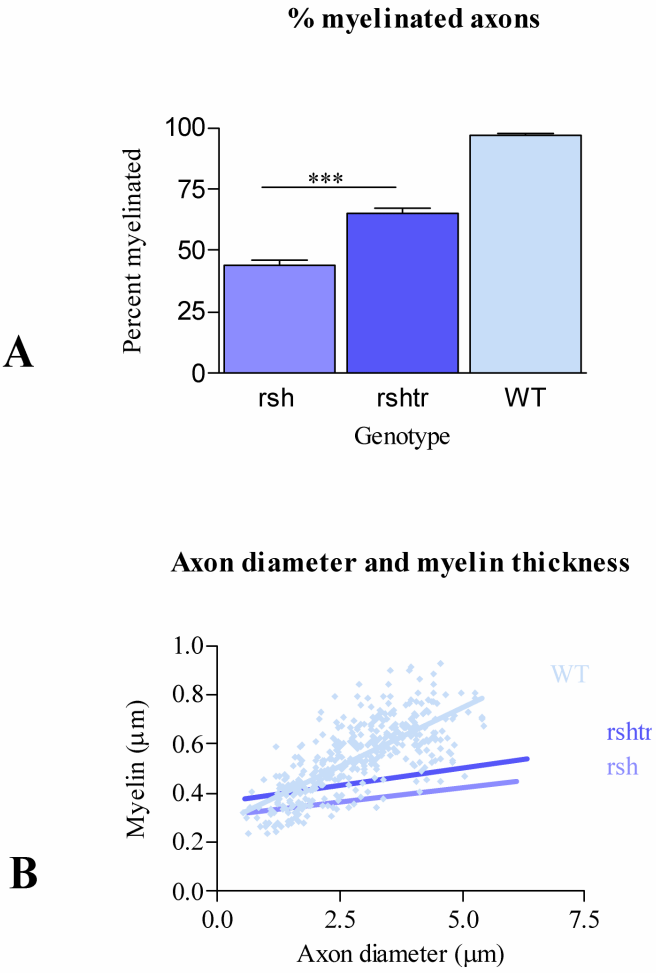

Figure7A. Graph of proportion of myelinated axons expressed as percentage of wild type. Counts performed on electron micrographs (x4000). *rumpshaker* (rsh) is reduced compared to transgene-complemented *rumpshaker* (rshtr) and both are reduced compared to wild type (WT).

Figure 7B. Graph of axon diameter plotted against myelin thickness. Increase in myelin thickness with increasing axon diameter is significantly reduced in *rumpshaker* (rsh) and transgene-complemented *rumpshaker* (rshtr). Individual points for wild type (WT) and regression lines for WT (slope 0.087) rsh (0.024) and rshtr (0.027) are shown.

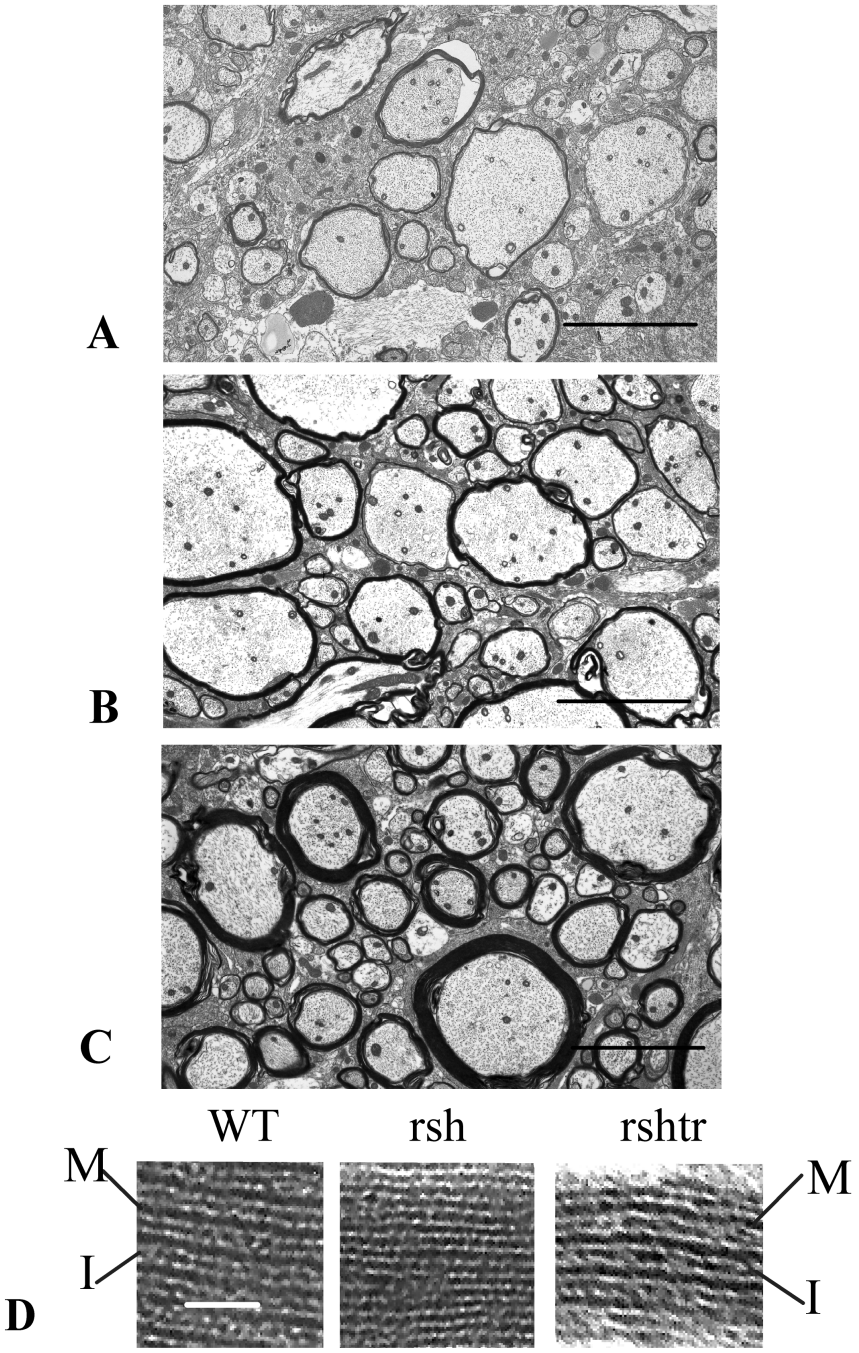

Figure 8. Electron micrographs of myelin sheaths (x 4000) from 70nm resin sections showing ventral column axons of cervical spinal cord at P20. **A**- *rumpshaker*- many axons are unmyelinated, myelin sheaths are very thin. **B**- transgene-complemented *rumpshaker*- most axons are myelinated although the myelin sheaths are still relatively thin. **C**- wild type-myelin sheaths are of the appropriate thickness for the diameter of axon. Bars =5µm **D**- micrograph montage of 70nm resin sections showing myelin periodicity in ventral column axons of cervical spinal cord at P20. Periodicity is altered in *rumpshaker* (rsh) and the major dense lines (M) and intraperiod lines (I) are indistinct, wild type (WT) and transgene-complemented *rumpshaker* (rshtr) show correct periodicity. Bar =20nm

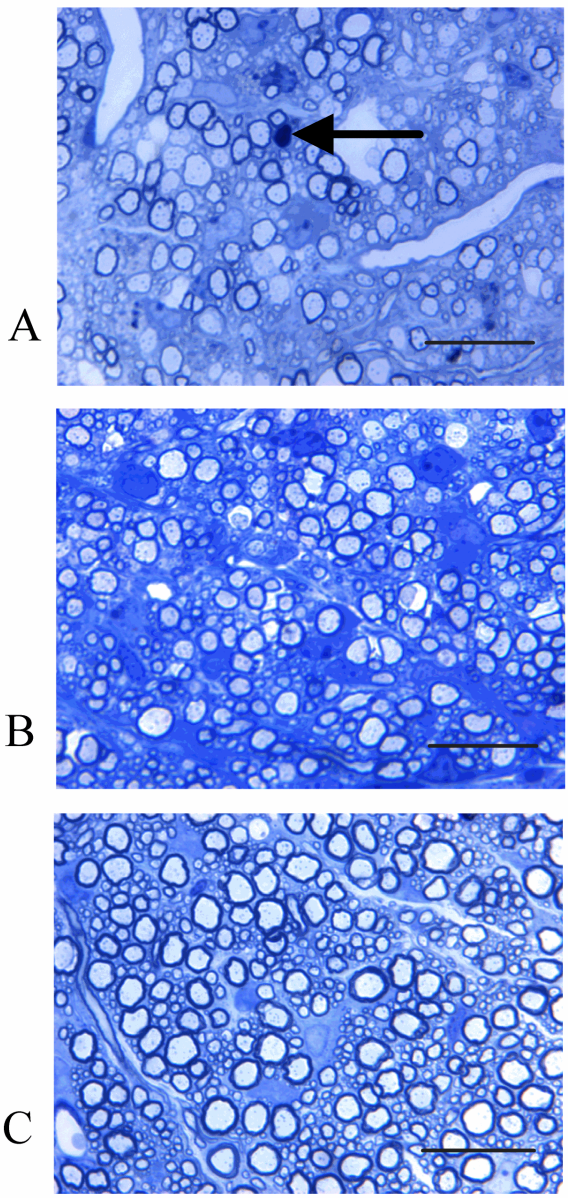

Figure 9. 1µm resin sections of the ventral columns of cervical spinal cord stained with methylene blue/azur II. **A** - *rumpshaker*, **B**- transgene-complemented *rumpshaker*, **C** -wild type. *rumpshaker* image shows prominent pyknotic nucleus (arrow) and many unmyelinated axons. Images x100 oil and bars= 20µm

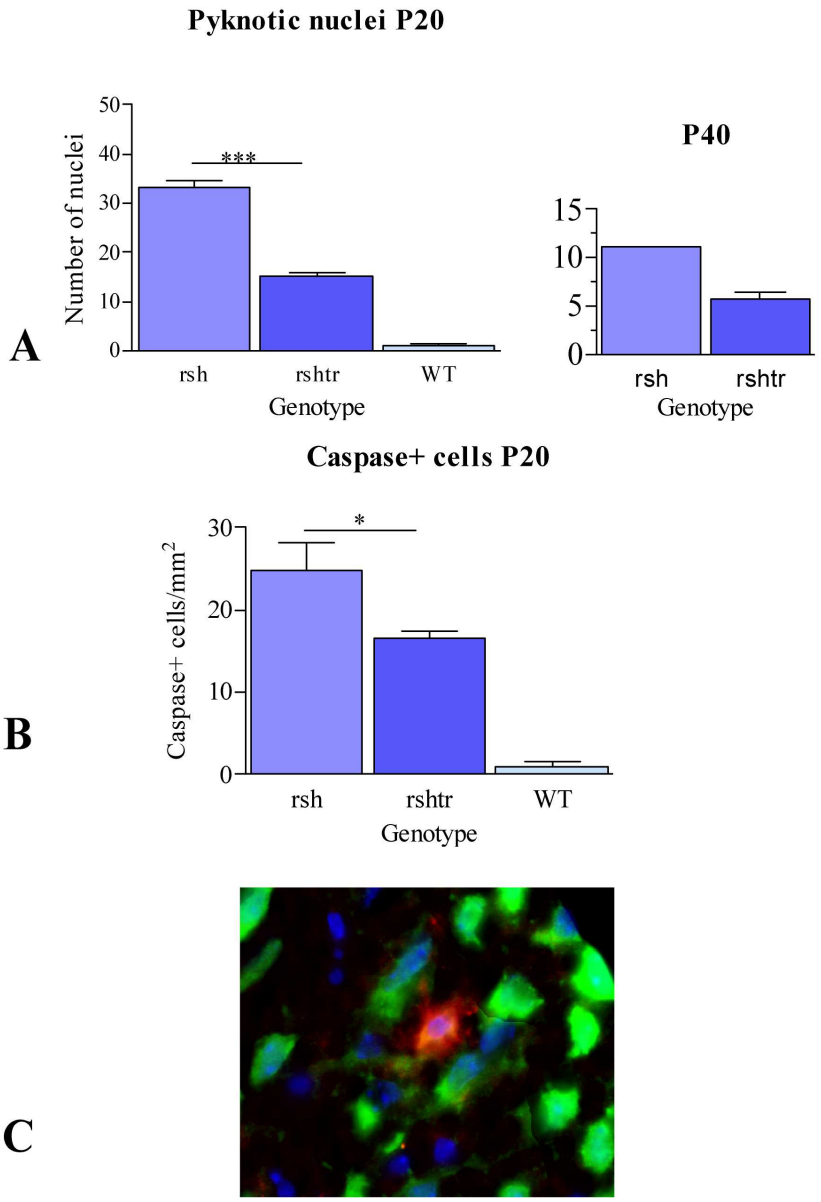

Figures 10A. Graphs depicting numbers of pyknotic nuclei counted in white matter tracts of cervical spinal cord at P20 and P40.Counts performed on 1µm resin sections. At each age the transgene-complemented *rumpshaker* (rshtr) is reduced compared to *rumpshaker* (rsh). P40 rsh n=1 (the only animal to survive to P40).
Figure 10B. Graph of caspase3 positive cell counts from the ventral columns of 15µm frozen sections. *rumpshaker* (rsh) has significantly greater numbers compared with transgene-complemented *rumpshaker* (rshtr). Wild type (WT) had only a nominal number of caspase3+ve cells.
Figure 10C. Image of ventral column of transgene-complemented *rumpshaker* immunostained for caspase3 (red) CC-1 (green) and the nuclear marker DAPI (blue) only one cell (orange) is positive for both caspase3 and CC-1

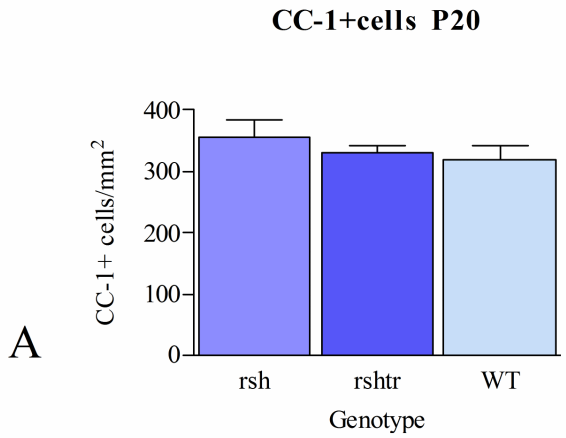

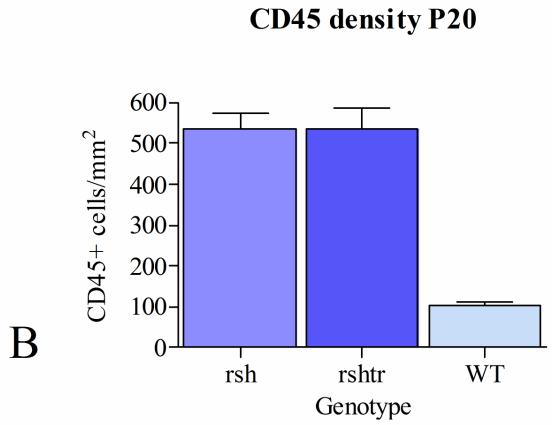

Figure 11A.Graph of CC-1+ve cell counts expressed as cells/mm^2. The counts were performed on 15µm frozen sections immunostained with CC-1, a marker for mature oligodendrocytes. The difference between the three genotypes was not significant

Figure 11B. Graph of inflammatory cell counts depicting CD45+ve cell counts expressed as positive cells/mm^2 performed on 15µm frozen sections. There is no difference between *rumpshaker* (rsh) and transgene-complemented *rumpshaker* (rshtr), each is significantly greater than wild type (WT).

4. Analyses of protein and mRNA levels in spinal cord and cultured oligodendrocytes

4.1 Introduction

PLP, the major myelin protein of the CNS (as discussed 1.4.2.4) is markedly reduced in the *rumpshaker* mouse on the C57BL/6 background (Al-Saktawi et al., 2003). In this study I analysed the level of PLP and the alternatively spliced isoform DM20 to determine if complementation of the mutant *Plp* gene with the wild type *Plp* gene would increase the levels of these proteins in the CNS myelin. Since other myelin proteins, such as MBP, are also reduced in the myelin extracts from the dysmyelinated *rumpshaker*, protein analyses of these were performed too. To ascertain if the same attenuation was reflected in the transcript level of the major myelin proteins, real time quantitative PCR was performed on total RNA extracted from P20 spinal cord.

4.2 Materials and methods

Myelin was extracted from dissected, snap frozen spinal cord following the method of Norton and Poduslo (1973a) previously described (2.5.1.), the myelin protein content assayed (2.5.3) and SDS PAGE Western blots performed (2.5.4). Enriched myelin fraction samples of *rumpshaker*, transgene-complemented *rumpshaker* and wild type P20 and P40 cord were blotted for the myelin proteins PLP, DM20, MBP, CNP and MAG. In addition total homogenate samples were blotted for GFAP and aspartoacylase (ASPA) and the pellet fraction enriched in membranes, including endoplasmic reticulum, blotted for the chaperone protein BiP. The NAD-dependent deacetylase Sirtuin2 was also investigated. Primary oligodendrocyte cultures (2.5.2) were lysed and the lysates blotted for PLP, MBP and ASPA. To perform real time quantitative PCR (qPCR) (2.6.2) and semi-quantatitive reverse transcriptase-PCR (RT-PCR), total RNA was extracted (2.6.1) following the instructions provided with RNAsol Bee reagent (Tel-Test Inc, Friendswood, Texas).

4.3 Results

4.3.1 Myelin protein analyses

PLP/DM20 level in *rumpshaker* myelin from P20 spinal cord is less than 20% of the level in wild type myelin. In the presence of the transgene (transgene-complemented *rumpshaker*), however, the level of PLP/DM20 recovers to near normal levels (approx 90% of wild type) (Figure 12A.). In contrast, the level of MBP in the presence of the transgene does not recover to normal levels, being only 30% of wild type, which was only slightly above the level of *rumpshaker* at 25%, a difference which is not statistically significant (Figure 12B.). Both CNP (Figure 13A.) and MAG (Figure 13B.) levels are improved from the low level in *rumpshaker*, but neither reaches the level of wild type. The oligodendrocyte culture lysates show similar results to the myelin fractions, the PLP/DM20 levels are very low in *rumpshaker* and recover to wild type levels in the transgene-complemented *rumpshaker* (Figure 14A.), whereas MBP is similarly low in the *rumpshaker* but does not recover in the transgene-complemented *rumpshaker* samples (Figure 14B.). Sirtuin2 levels were low in the *rumpshaker* but returned to normal in the transgene-complemented *rumpshaker* samples (Figure 12c.).

4.3.2 Non myelin proteins

Total homogenate fractions were blotted for GFAP, a marker for astrocytes and ASPA, a protein marker for oligodendrocytes. In both the *rumpshaker* and transgene-complemented *rumpshaker* animals GFAP levels are elevated compared to wild type (Figure 15A.); in contrast, the ASPA levels are reduced compared to wild type (Figure 15B.). Results for the endoplasmic reticulum enriched pellet fraction blotted for BiP are discussed in (5.3.1)

4.3.3 Real time PCR (qPCR)

Total RNA from wild type, *rumpshaker* and transgene-complemented *rumpshaker* cord was collected and real time PCR performed for *Plp/Dm20* and *Mbp* mRNA. The level of *Plp/Dm20* mRNA has returned to near wild type level in the transgene-complemented *rumpshaker* samples (Figure 16A). *Mbp* mRNA levels in both *rumpshaker* and transgene-complemented *rumpshaker* remains 20% lower than those of wild type (Figure 16B).

4.4 Discussion

In this section I have presented data showing that in the presence of the wild type transgene both PLP/DM20 and *Plp/Dm20* are returned to near wild type levels. Conversely, MBP is not returned to normal levels in the transgene-complemented *rumpshaker* animals, remaining at a similar level to *rumpshaker,* the same result is reflected in the oligodendrocyte cultures, which do not elaborate a myelin sheath, suggesting that the paucity of myelin is not the cause of the continued reduction in MBP. *Mbp* mRNA levels are also reduced compared to wild type, however this reduction is not nearly as great as the protein, suggesting that the deficiency in MBP occurs predominantly during translation or post-translational modification as a consequence of altered translation efficiency, accelerated degradation or a combination of the two. CNP and MAG levels have a greater recovery than MBP but again do not return to wild type levels. These proteins employ similar but distinct transport mechanisms to PLP suggesting that a global protein transport deficit is not induced and that the selective attenuation of MBP is a specific effect. Sirtuin2 levels mirrored those of PLP in that they were recovered to normal in the transgene-complemented *rumpshaker* cord. In both the *rumpshaker* and transgene-complemented *rumpshaker* animals ASPA is reduced whilst GFAP is elevated.

While the numbers of oligodendrocytes between all three genotypes are similar, the density of astrocytes and microglia are increased in *rumpshaker* and transgene-complemented *rumpshaker*. The elevation in the density of these cell types will have a significant dilutional effect on the oligodendrocyte-derived proteins that are present in the total homogenate. This could account for the reduction in the ASPA content despite the number of oligodendrocytes being maintained. The elevation in GFAP is most likely a mild astrocytosis.

This study reveals that sirtuin 2 is grossly reduced in *rumpshaker* myelin and recovered to wild type levels in the transgene-complemented *rumpshaker*. Sirtuin 2 is targeted to the paranodal region of the myelin sheath (Southwood et al., 2006). Werner et al show that in the PLP ^{null} mouse sirtuin 2 was “virtually absent” and surmised that PLP/DM20 was required to transport sirtuin2 to the myelin. They hypothesise that the late-onset axonal degeneration observed in the PLP ^{null} mice may be associated with the absence of sirtuin 2,

that it has a function in the support of the axon by the oligodendrocyte (Werner et al., 2007).

Although the major myelin protein PLP/DM20 is recovered in the transgene-complemented *rumpshaker* animals, severe dysmyelination still persists, suggesting that merely replacing or "topping up" the aberrant PLP/DM20 with wild type protein is not enough to establish the synthesis of normal amounts of myelin, that other mechanisms, not ameliorated in the transgene-complemented *rumpshaker*, cause the dysmyelination to persist.

rumpshaker PLP is present in the oligodendrocyte membrane as evidenced by positive immunostaining with the conformational sensitive antibody, O10; however, processing of the mutant protein is altered. McLaughlin(McLaughlin et al., 2006) demonstrated that *rumpshaker* PLP has an accelerated degradation through the MG132 sensitive proteasome, being two times faster than wild type. Furthermore, the mutant protein is endocytosed from the membrane at a faster rate than wild type (McLaughlin et al unpublished data). It is possible that the high turnover of a major myelin component renders the myelin sheath unstable, or that the turnover is too fast to allow accumulation and thickening of the myelin sheath.

The association of PLP with myelin is dependant on several factors, which could be affected when a misfolded protein is present. PLP is transported to the myelin membrane by association with glycosylceramide/cholesterol enriched microdomains known as lipid rafts (Simons et al., 2000). It has been shown that the cholesterol composition of *rumpshaker* myelin is compromised, perhaps affecting the lipid raft formation or the ability of PLP to associate with them (Karthigasan et al., 1996; Kramer-Albers et al., 2006) Palmitoylation, a post translational modification of PLP, is necessary for stabilisation of the protein–lipid interaction Schneider (Schneider et al., 2005) and Tetzloff (Tetzloff & Bizzozero, 1998) concluded that acylation plays an important role in the acquisition of palmitic acid by PLP. The abnormal molecular organization of *rumpshaker* PLP may prevent these post-translational modifications.

The continued reduction in MBP, which is essential for myelin formation, may also be critical in the continuing dysmyelination (Shine et al., 1992). *Mbp* mRNA is translocated to the cytoplasmic face of the major dense line where it is translated on free ribosomes and where its efficient translation requires a stabilising mRNA protein complex. Increased citrullination, a post-translational modification of MBP, decreases the ability of the protein

to aggregate with acidic lipid vesicles (Seiwa et al., 2000). Fyn tyrosine kinase (Fyn) is a signalling molecule which stimulates MBP gene transcription and has a putative role in the initiation of myelination (Umemori et al., 1999). Fyn deficient mice have been shown to have increased citrullination of MBP; moreover, L-MAG, which remains reduced in the transgene-complemented *rumpshaker* animals, stimulates the activation of Fyn. This is perhaps too simplistic an explanation and would certainly require further investigation; however, it may contribute to the loss of the synchronised synthesis of myelin.

An ongoing study within our laboratory has utilised transgenic complementation to produce *rumpshaker* mice harbouring a transgenic cosmid containing one copy of the *Mbp* gene to determine if additional MBP affects an improvement in phenotype, a further cross under investigation is the *rumpshaker* x *shiverer* (*shi*). It is hoped that these studies will elucidate further the relationship between PLP and MBP.

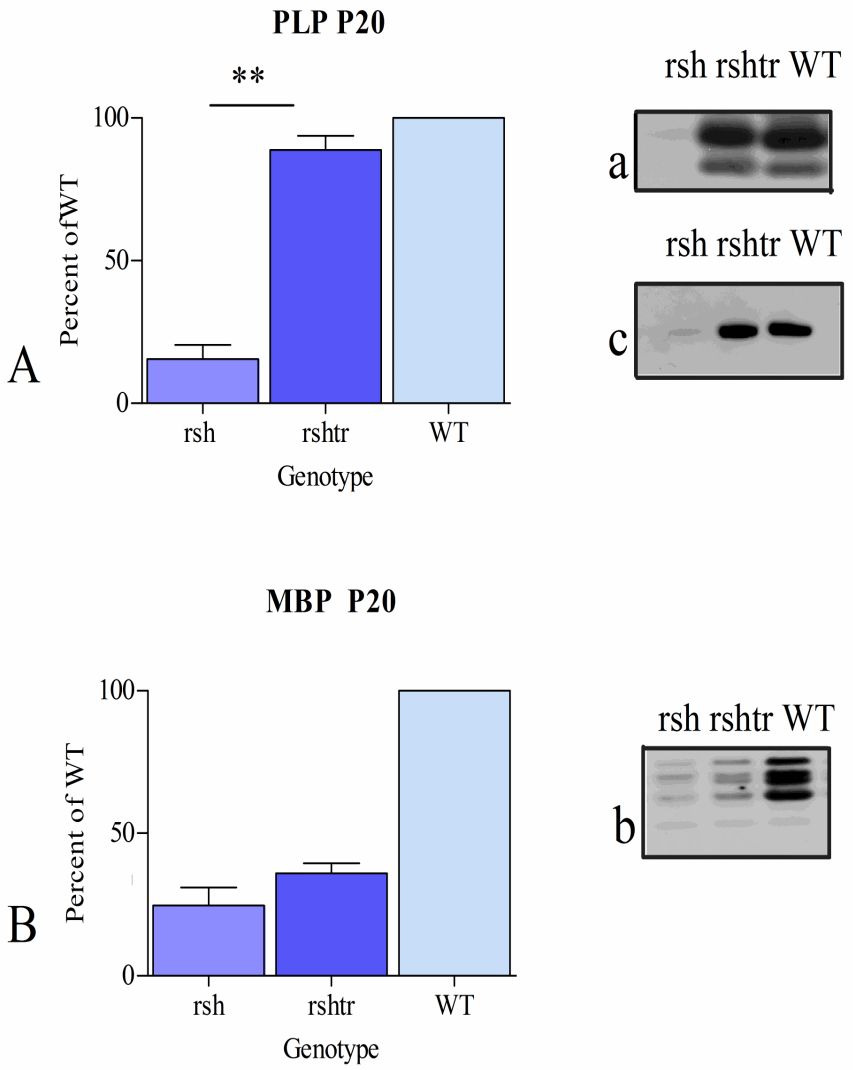

Figure 12A. Graph of PLP protein in myelin fraction of P20 cord expressed as a percentage of wild type. *rumpshaker* (rsh) is approx 20% of wild type (WT) whereas transgene-complemented *rumpshaker* (rshtr) is recovered to near wild type. Figure 12a. Representative blot stained with anti-PLP/DM20 (transgene-complemented *rumpshaker* and wild type are necessarily saturated to allow detection of *rumpshaker* band), Figure 12c. Blot of sirtuin 2 showing recovery of sirtuin 2 in the transgene-complemented *rumpshaker*. Figure 12B. Graph of MBP protein in myelin fraction of P20 cord expressed as a percentage of wild type. Transgene-complemented *rumpshaker* does not recover to wild type levels, remaining only slightly elevated when compared to *rumpshaker*, The difference is not statistically significant. Figure 12b. PVDF membrane of the myelin fraction blotted with anti-MBP.

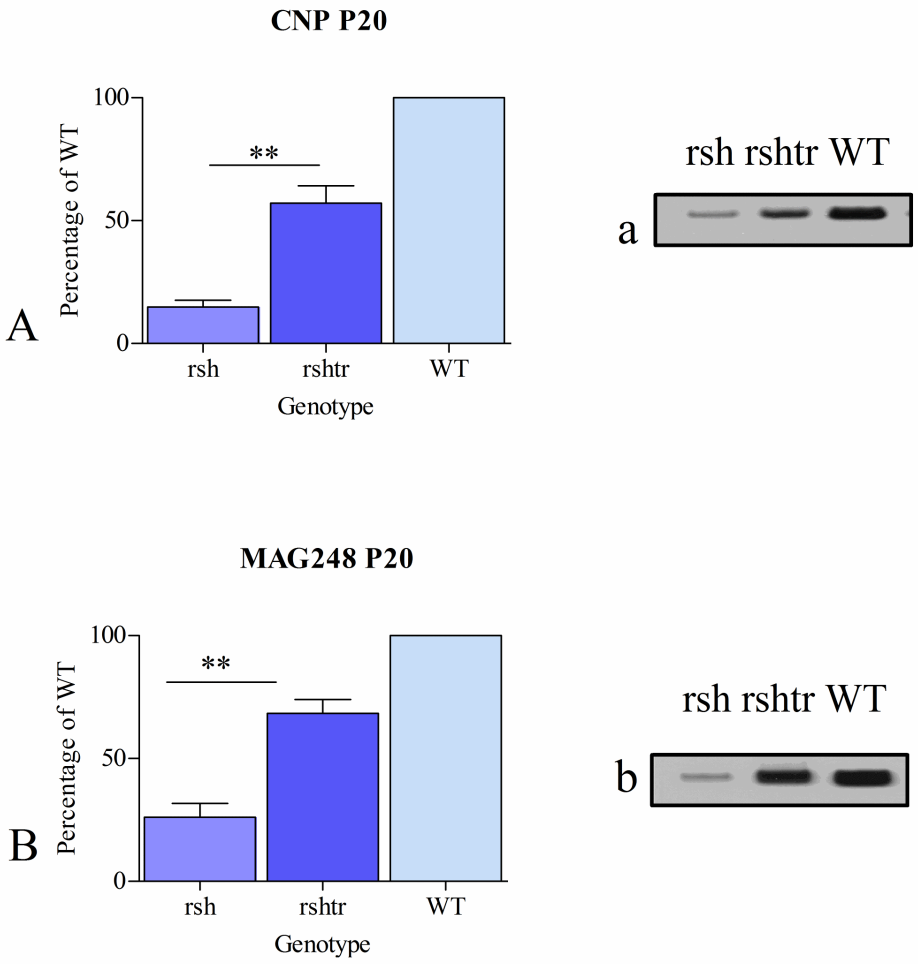

Figure 13A. Graph of CNP protein in myelin fraction of P20 cord expressed as a percentage of wild type. Transgene-complemented *rumpshaker* is partially recovered. Figure 13a. Panel shows representative CNP blotFigure 13B. Graph of MAG protein in myelin fraction of P20 cord expressed as a percentage of wild type. Transgene-complemented *rumpshaker* is partially recovered. Figure 13b. Panel shows representative MAG blot.

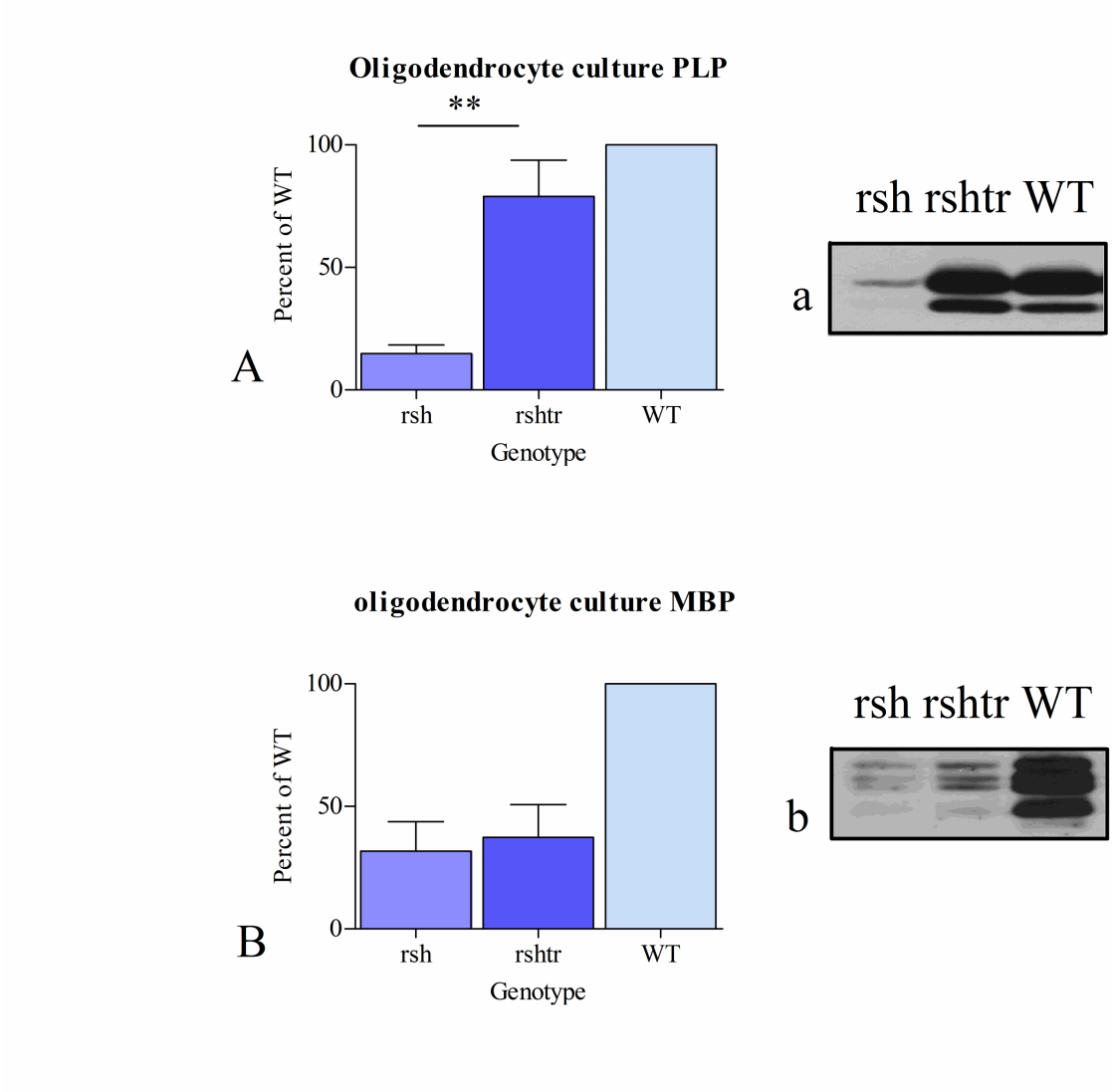

Figure 14A. Graph of PLP/DM20 protein from oligodendrocyte cell culture lysate expressed as a percentage of wild type. Transgene-complemented *rumpshaker* is returned to near wild type levels. Figure 14a. Panel shows western blot PVDF membrane blotted with anti-PLP.

Figure 14B. Graph of MBP protein from oligodendrocyte cell culture lysate expressed as a percentage of wild type. Transgene-complemented *rumpshaker* remains at a similar level to *rumpshaker;* the difference is not statistically significant. Figure 14b. Representative panel of membrane blotted with anti-PLP.

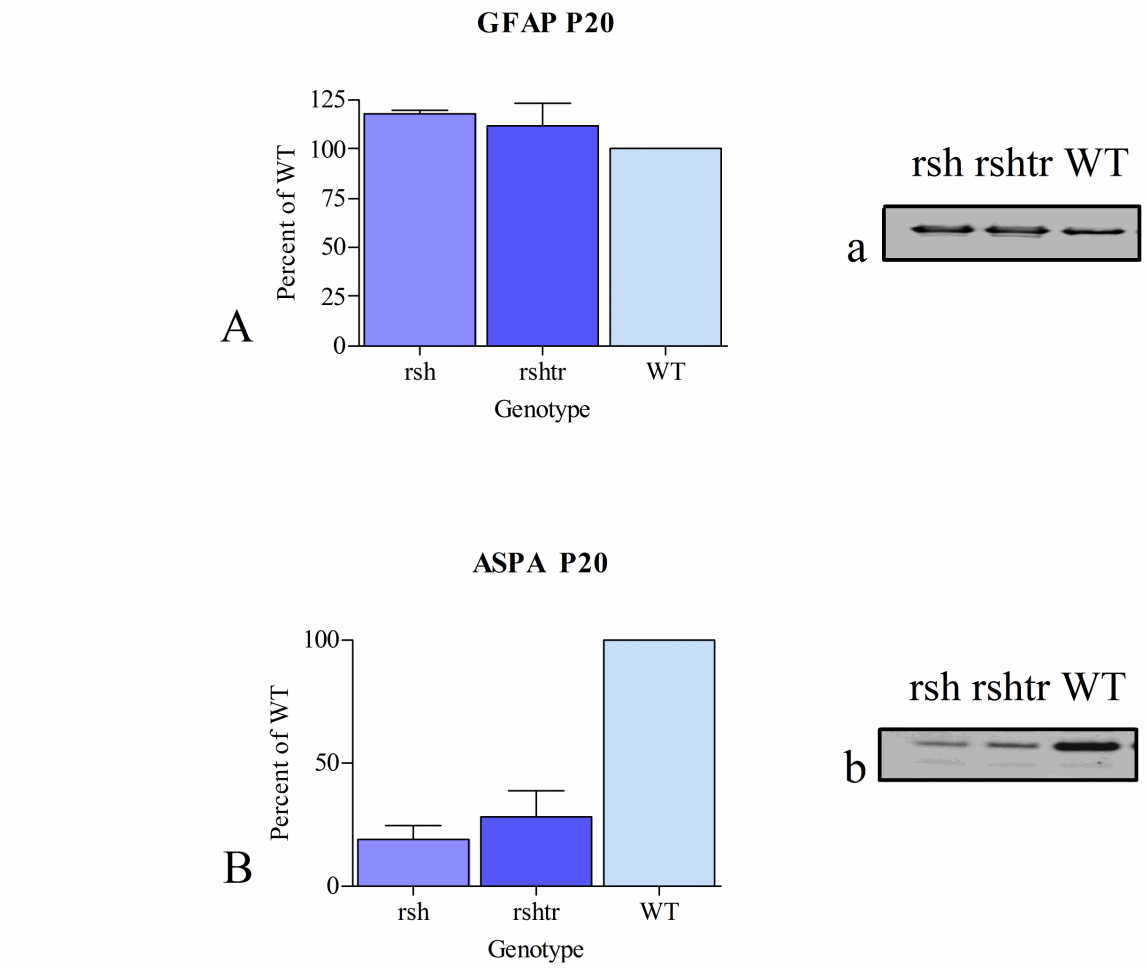

Figure 15A. Graph of GFAP protein expressed as a percentage of wild type in total homogenate of P20 cord. GFAP is elevated in both *rumpshaker* and transgene-complimented *rumpshaker* compared to wild type. Figure 15a. Representative western blot of GFAP.

Figure 15B. Graph of ASPA protein expressed as a percentage of wild type in total homogenate of P20 cord. ASPA is significantly lower in both *rumpshaker* and transgene-complimented *rumpshaker* compared to wild type but not significantly different from each other. Figure 15b. Panel shows representative blot stained with ASPA.

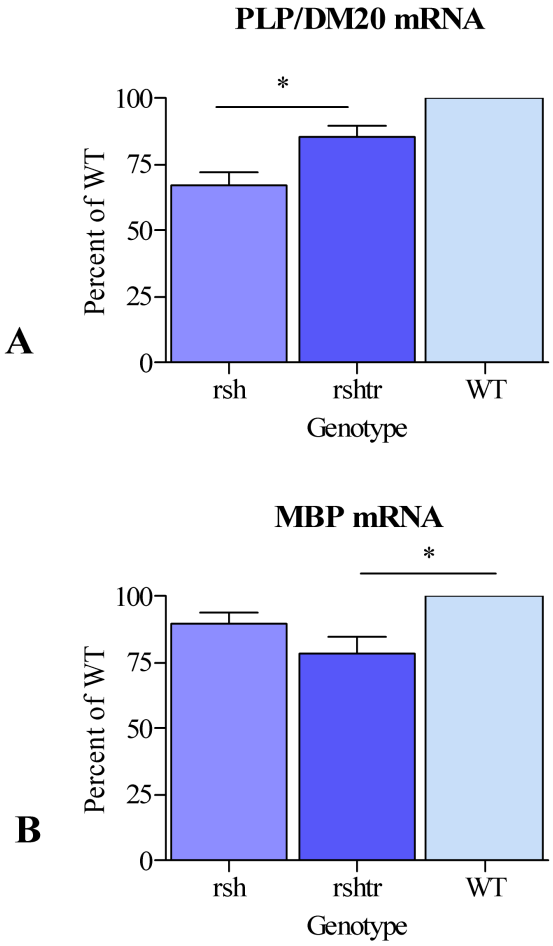

Figure 16A Graph of *Plp/Dm20* mRNA from P20 cord expressed as a percentage of wild type. *Plp/Dm20* message in transgene-complemented *rumpshaker* is significantly increased to near wild type levels.

Figure 16B Graph of *Mbp* mRNA from P20 cord expressed as a percentage of wild type. *Mbp* message in transgene-complemented *rumpshaker* remains around 20% lower than wild type.

5. Study of the unfolded protein response

5.1 Introduction

The unfolded protein response (UPR) is a complex signal transduction system activated in response to the accumulation of misfolded proteins within the endoplasmic reticulum lumen (Gow, 2004). It is part of the endoplasmic reticulum stress response comprising the UPR, the endoplasmic reticulum associated degradation (ERAD) pathway and the endoplasmic reticulum overload response, that together act to protect the cell and subsequently the organism from the effects of an accumulation of unfolded or misfolded proteins. Within the membrane of the endoplasmic reticulum (ER) are three sensors, PERK (PKR-like resistant kinase), ATF6 (activating transcription factor 6) and IRE1 (Inositol requiring enzyme 1) that monitor the accumulation of unfolded proteins and activate the ER stress response when these become a burden upon the cell.

There are many proteins and transcription factors associated with the UPR, which modulates cell homeostasis through transcription and repression of translation. Previous studies have shown that the UPR is activated in the *rumpshaker* (McLaughlin et al., 2007), most likely in response to the accumulation of the misfolded PLP. This study sought to reveal any alteration in the activation status of the UPR in response to the introduction of the wild type PLP transgene. I investigated the molecular chaperone protein BiP and the transcription factors *Chop*, *Atf3* and *Xbp1* as these are key indicators of an unfolded protein response.

5.2 Materials and methods

The pellet fractions from spinal cords of P20 mice, processed by the method of Norton and Poduslo (2.5.1), were collected and resuspended in 0.25M sucrose. SDS-PAGE was performed on the samples and the nitrocellulose membrane blotted with anti-BiP. mRNA from whole cord was prepared (2.6.1) and RT-PCR performed (2.6.4) using primers for the amplification of *Chop*, *ATF3* and *XBP1*.

5.3 Results

5.3.1 BiP

The level of the immunoglobulin binding protein BiP (also known as Glucose-regulated protein 78(GRP78)) is elevated in both the *rumpshaker* and transgene-complemented *rumpshaker* samples compared to wild type; the transgene-complemented *rumpshaker* level is significantly higher than *rumpshaker* (Figure 17A).

5.3.2 XBP1

A small amount of active (spliced) *Xbp1* mRNA is present in the samples of both *rumpshaker* and transgene-complemented *rumpshaker*, although the majority is unspliced. The wild type sample consists entirely of unspliced *Xbp1* (Figure 17B.).

5.3.3 Chop and ATF3

Both *Chop* (Figure 18A.) and *ATF3* (Figure 18C.) mRNAs are elevated in *rumpshaker* and transgene-complemented *rumpshaker* samples compared to wild type; there is no significant difference between samples from the two mutants.

5.4 Discussion

Results from the study of the unfolded protein response show that *Chop*, *Atf3*, *Xbp1* and BiP were elevated in both *rumpshaker* and transgene-complemented *rumpshaker* mutants compared to wild type. The difference between both mutants in each case was not significant with the exception of BiP. This study revealed that there is increased induction of BiP in the transgene-complemented *rumpshaker* compared to *rumpshaker*.

The ER is the site for the synthesis of secretory and membrane proteins and lipids and is also a major intracellular calcium storage compartment and as such ER homeostasis is of the utmost importance to the survival of the cell. BiP is a stress-inducable ER chaperone protein that binds to unfolded peptides and promotes proper folding of newly synthesised proteins. It also acts as the master modulator of the UPR network and under normal conditions binds to the luminal domain of the ER stress sensors PERK, ATF6 and IRE1 inhibiting their activation. Upon ER stress BiP dissociates from the stress transducers and

binds to the accumulating unfolded proteins, the unbound transducers become active leading to the transcriptional and translational induction of various intermediaries resulting in upregulation of CHOP (Oyadomari & Mori, 2004). It is disputed whether the effect of the transcriptional activation of CHOP is pro-apoptotic or anti-apoptotic. McLaughlin et al reported an increase in CHOP positive nuclei in *rumpshaker* when expressed on the C57 background, a result which correlates with the increased number of apoptotic cells in these animals (McLaughlin et al., 2007), and one which would suggest a pro-apoptotic role. Interestingly, they failed to co-immunostain CHOP and Caspase3 perhaps indicating that different cells were involved or that the temporal expressions of the proteins were different. Additionally, Marciniak reports that the deletion of CHOP protects cells from ER stress by decreasing the client protein load (Marciniak et al., 2004). Conversely, Southwood (Southwood et al., 2002) showed that CHOP null/*rsh* mice died earlier than *rumpshaker* controls, suggesting a protective role for CHOP. Rao in his review refers to CHOP as an ER stress-induced cell death modulator (Rao et al., 2004) which is perhaps cell type specific. The elevation in *Chop* transcription in both the *rumpshaker* and transgene-complemented *rumpshaker* would suggest a pro-apoptotic function; however, since no change is induced by the introduction of the transgene we cannot deduce anything further from the results. Likewise, we see no change in the level of *Atf3*, the induction of which has been shown to increase the likelihood of an apoptotic event. Recently it has been reported that this transcription factor plays a minor role in the UPR and that its activation is a secondary event unrelated to cell death (Sharma et al., 2007).

Activation of IRE1 mediates the splicing of X-box binding protein pre-messenger RNA to form mature *Xbp1* mRNA. The transcription factor protein XBP-1(S) translated from the mature mRNA binds to, among other things, the ER stress response element (ERSE) activating the transcription of ER chaperones like BiP (Yoshida et al., 2006). In both the *rumpshaker* and transgene-complemented *rumpshaker* we detected a small amount of mature *Xbp1* mRNA (spliced) however the majority remained unspliced. Lee et al reported that the expression of BiP was only modestly dependant on XBP-1 (Lee et al., 2003). Recently Yoshida et al demonstrated that unspliced pre-mRNA encodes a functional protein the expression of which is significantly induced during recovery from ER stress (Yoshida et al., 2006), they also demonstrated a corresponding increase in unspliced mRNA. The cellular response to chemically induced ER stress, such as that employed by Yoshida, is many times greater than that induced in vivo. It is not unreasonable to surmise that there may be a recovery response in the transgene-complimented *rumpshaker* that we have failed to detect.

BiP plays a central role in the UPR. As an ER chaperone protein, an integral part of the "ER quality control system" it assists in the folding of client proteins and retains misfolded proteins within the ER. In addition it acts as a stress sensor, its dissociation from PERK results in attenuation of protein synthesis reducing the client protein load in the cell, and dissociation from IRE1 and ATF6 activates transcription of ER chaperone proteins and *Xbp1* (S). Gülow et al demonstrated that BiP expression is tightly controlled at post-transcriptional level, and that under ER stress conditions translation efficiency is enhanced (Gülow et al., 2002), an essential response if the cell is to survive. Recent studies have suggested that ER stress causes BiP (or a subpopulation of) to redistribute from the ER lumen to become an ER transmembrane protein where it forms a complex with caspase-7 and caspase-12 at the ER surface preventing caspase cascade activation and subsequent cell death (Rao et al., 2004). It can be said that the anti-apoptotic role of BiP represents an important pro-survival component within the UPR. It seems entirely possible that this element has been upregulated in the transgene-complemented *rumpshaker*, which has a larger elevation in BiP and lower numbers of caspase-3 positive cells than *rumpshaker* (3.3.3.4). Perhaps the burden of wild type PLP in addition to the misfolded PLP has induced an increase in translation of BiP, which has had the added benefit of reducing oligodendrocyte apoptosis. Karim et al found no induction of the UPR in #66 hemizygote animals which are essentially transgene-complemented *rumpshaker* without the *rumpshaker* mutation (unpublished data), it is apparent therefore that the continuing presence of misfolded *rumpshaker* PLP, even at the reduced level in transgene-complemented *rumpshaker,* induces activation of the unfolded protein response.

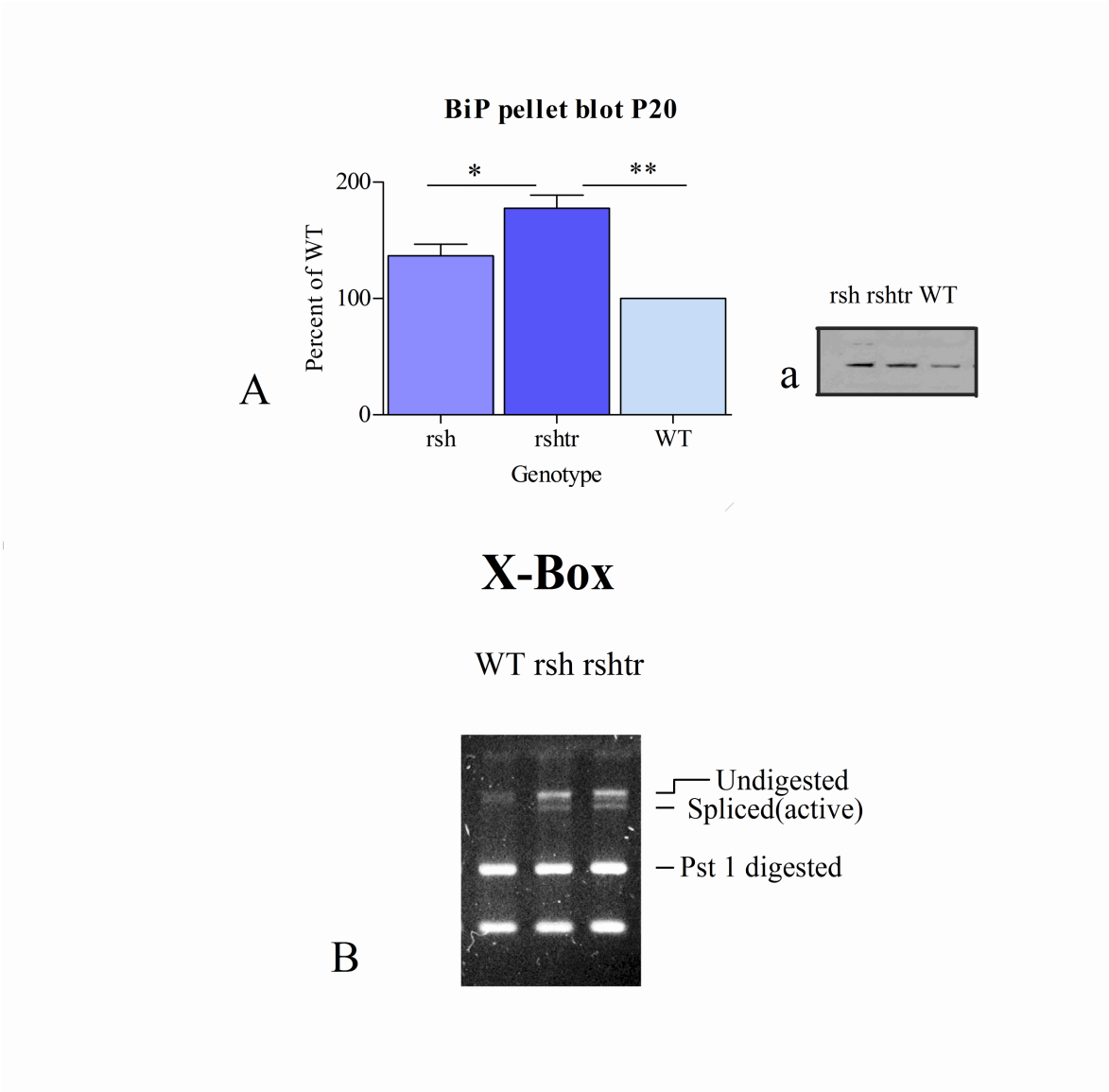

Figure 17A. Graph of BiP protein from pellet fraction of P20 cord expressed as a percentage of wild type. BiP is elevated in *rumpshaker* compared to wild type but the transgene-complemented *rumpshaker* is elevated when compared to *rumpshaker* . Figure 17a. Representative blot of BiP

Figure 17B. *Pst1* digested X-Box protein PCR products. *Rumpshaker* (rsh) and transgene-complemented *rumpshaker* (rshtr) have undigested and spliced bands as well as a *Pst1* digested band, wild type product is completely digested.

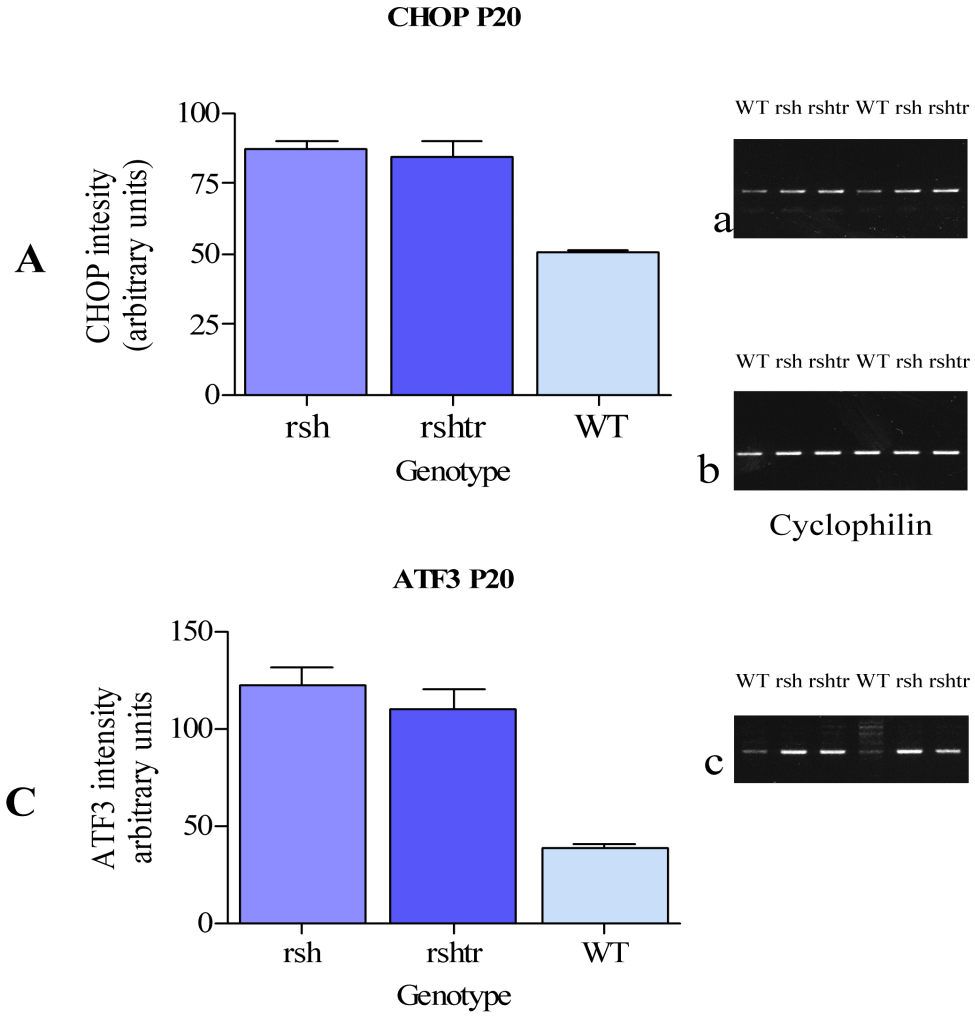

Figure 18A. Graph of quantified agarose gel products of RT-PCR, using primers for CHOP against cDNA from P20 cord showing both *rumpshaker* and transgene-complemented *rumpshaker* are elevated with no significant difference between them.

Figure 18a. Image of representative agarose gel of RT-PCR CHOP products

Figure 18b. Image of cyclophilin gel an internal control showing equal loading

Figure 18C. Graph of quantified agarose gel from RT-PCR, performed using primers for ATF3 against cDNA from P20 cord. Again, both *rumpshaker* and transgene-complemented *rumpshaker* are elevated with no difference between them.

Figure 18c. Image of representative agarose gel of RT-PCR ATF3 products.

6. Summary and further work

This body of work was carried out to determine if the introduction of wild type PLP/DM20, by transgenic complementation, into *rumpshaker* on the C57BL/6 background would ameliorate the lethal phenotype, elucidate the primary cause of oligodendrocyte apoptosis and establish the cause of premature death. There are several possible explanations for the lethal phenotype, which may act in tandem.

Rumpshaker mice harbouring the wild type transgene survive up to, and possibly beyond, postnatal day 40, significantly longer than *rumpshaker*. There is an increase in myelin volume and density and in the number of myelinated axons in the presence of wild type PLP. In addition, the periodicity of the myelin is returned to that of wild type, having distinct intraperiod and major dense lines.

It is possible that with an increased number of myelinated axons the transgene-complemented *rumpshaker* attains a critical threshold of myelination and that essential neuronal pathways, for example, the respiratory control centre, are sufficiently myelinated to allow survival. Miller et al (Miller et al., 2003) reported severe dysmyelination of the respiratory control centre in the *md rat* leading to “lethal hypoxic depression of breathing” around the time of premature death in these animals, further investigation would be required to determine if this is an explanation for the seizures which may be the cause of premature death in *rumpshaker* and if transgene-complementation improves the incidence or severity of the seizures.

The presence of misfolded PLP within the *rumpshaker* myelin causes a change in the myelin structure revealed by the altered periodicity. The presence of the misfolded PLP may affect the arrangement of key components in the process of myelination such as cholesterol and glycosphingolipids (Karthigasan et al., 1996). Processing of key myelin proteins is altered in both *rumpshaker* and transgene-complemented *rumpshaker*. McLaughlin demonstrated that *rumpshaker* PLP is endocytosed from the myelin membrane at an increased rate perhaps causing the sheath to be unstable and preventing it from reaching full maturity (unpublished data). PLP/DM20 levels in the transgene-complemented *rumpshaker* myelin are returned to wild type levels but MBP remains severely reduced and CNP and MAG only partially recover. Transgene-complementation of *rumpshaker* returns the myelin to normal periodicity and although myelin volume,

density and the number of myelinated axons are increased it is still significantly dysmyelinated. The presence of abnormal myelin has consequences for the underlying axon. Studies by Edgar (Edgar et al., 2004; Edgar & Garbern, 2004) confirmed that the oligodendrocyte directly supports the underlying axon although it is not yet clear how this is achieved, perhaps the presence of normal amounts of PLP within the myelin and/or the increased stability of the myelin sheath is improving the feedback control to the axon. Trajkovic reported that transport of PLP to the myelin sheath is under neuronal control (Trajkovic et al., 2006) this too could be improved by the presence of wild type PLP.

The presence of the misfolded *rumpshaker* PLP within the oligodendrocyte elicits the unfolded protein response. Investigation of several components within the UPR revealed that only the molecular chaperone protein BiP was altered, being upregulated in transgene-complemented *rumpshaker*. At a cellular level, the presence of the wild type transgene reduces the number of apoptotic oligodendrocytes, it is possible that upregulation of BiP is reducing stress within the oligodendrocyte and thus reducing apoptosis.

The microglia/macrophage response in transgene-complemented *rumpshaker* is unchanged remaining at a level five times greater than wild type. Further investigation would be required to establish the cause of this inflammation. Is the microglial/macrophage activation a response to the presence of myelin debris, or does activation of the inflammatory response produce cytokines, which induce the apoptosis? Lin demonstrated that apoptosis following ER stress was related to release of the immune cytokine interferon-γ in oligodendrocyte culture (Lin et al., 2005); alternatively, low level or transient cytokine release can be protective (Vilhardt, 2005).

Transgene-complementation of the *rumpshaker* with wild type PLP has rescued, to a degree, the lethal phenotype. Further studies will be required to determine why these animals survive and conversely why *rumpshaker* animals die. Breeding pairs have been set up to ascertain the longevity of the transgene-complemented *rumpshaker*. In addition proteomic studies are being conducted utilising mass spectrometry to determine the ratio of *rumpshaker* to wild type PLP within total homogenate samples of P20 spinal cord. Clearly, there are many more questions which remain unanswered, transgenic complementation provides a useful tool to address many of these.

7. Appendix

7.1 Tissue fixation and immunocytochemistry

7.1.1 APES coated slides

Coating microscope slides with the adhesive APES (3(aminopropyl)triethoxysilane) (Sigma) enabled the sections to adhere to the slides during the subsequent steps in immunohistochemistry. Slides were soaked overnight in 5% Decon 90 (Decon Lab Ltd) washed in distilled water and oven dried. The dried slides were dipped in methylated spirit then soaked in 0.25% APES/methylated spirit for 2 minutes, rinsed in distilled water, oven dried and wrapped in foil. APES-coated slides were stored at room temperature.

7.1.2 Karnovsky's modified fixative

8% Paraformaldehyde:

20 g of paraformaldehyde was added to 250 ml of dH2O and heat to 65°C.

A few drops of 1M NaOH added to clear the solution which was allowed to cool.

0.08M Cacodylate buffer:

17.1224g sodium cacodylate dissolved in 1 litre of dH2O and adjusted to pH 7.2.

Preparation of Karnovsky fixative (500ml)

250ml 8%Paraformaldehyde
100ml 25% EM Grade glutaraldehyde
150ml 0.08M sodium cacodylate buffer
0.25g calcium chloride
Add volumes, dissolve calcium choride, adjust to pH 7.2, filter, and store at 4ºC.

7.1.3 4% paraformaldehyde

20g paraformaldehyde was added to 500ml PBS and heated to 65°C. A few drops of 1M NaOH were added to clear the solution which was then cooled and filtered.

7.1.4 Periodate-lysine-paraformaldehyde fixative(P-L-P)

Buffered lysine solution:

13.7g lysine monohydrate dissolved in 375ml dH2O.
1.8g sodium hydrogen phosphate dissolved in 100ml dH2O.
The two solutions were mixed to give 475ml and pH 7.4

10% Paraformaldehyde:

20g paraformaldehyde dissolved in 200 ml dH2O and heated to 65°C. Few drops of 1M NaOH were added to clear and allowed to cool and filtered.

Preparation of P-L-P fixative:

Immediately before use the buffered lysine solution was added to the 10% paraformaldehyde and the volume made up to 1 litre using 0.1M phosphate buffer. Finally 2.14g sodium periodate was dissolved in the solution.

7.1.5 Phosphate buffer saline (PBS)

8g Sodium Chloride
1.44g Disodium hydrogen phosphate
0.24g potassium dihydrogen phosphate
0.2g potassium chloride
Dissolved in 800 ml of dH2O, adjusted to pH 7.4 with 1M HCl and the volume made up to 1 litre with dH2O

7.2 Tissue processing and staining for Electron Microscopy

7.2.1 Resin processing

The following is the programme entered into the Lynx tissue processor in order to produce resin blocks from the Karnovsky fixed tissue.

1-	isotonic cacodylate buffer	50 min	4°C
2-	1% OsO4 in cacodylate buffer	2hr	room temperature
3-	isotonic cacodylate buffer	30 min	room temperature
4-	50% ethanol	5 min	4°C
5-	50% ethanol	10 min	4°C
6-	70% ethanol	5 min	4°C
7-	70% ethanol	10 min	4°C
8-	80% ethanol	5 min	4°C
9-	80% ethanol	10 min	4°C
10-	90% ethanol	5 min	4°C
11-	90% ethanol	10 min	4°C
12	ethanol	20 min	4°C
13	ethanol	20 min	4°C
14-	propylene oxide	15 min	room temperature
15-	propylene oxide	15 min	room temperature
16-	1:3 resin: propylene oxide	13 hr	room temperature
17-	1:1 resin: propylene oxide	18hr	room temperature
18-	resin	6hr	30ºC

7.2.2 Araldite Resin

30g Araldite CY212

25.2g DDSA (Dodecynyl succinic anhydride)

1.2ml DMP 30 (2,4,6tri(dimethylaminoethyl)phenol

0.75ml Dibutylphthalate

7.2.3 Methylene blue/ azur II *stain*

1% Methylene blue powder

1% azur II powder

1% Disodium tetraborate

dissolved in distilled H_2O and filtered before use

7.2.4 Staining of Electron microscope grids

Reynold's lead citrate (1.2mM lead citrate, 1.8mM sodium citrate, pH 12.0)

1- 1.33 g lead nitrate dissolved in 15 ml dH_2O 1 min vigorous shaking
2- 1.76 g sodium citrate dissolved in 15 ml dH_2O 1 min vigorous shaking
Add solution 1 to solution 2 and equilibrate over 30 minutes with occasional shaking.

Clear with 1M NaOH and make up to the final volume of 50 ml with dH2O.

Saturated Uranyl acetate

Uranyl acetate in excess dissolved in 50% ethanol (store at 4°C in the dark)

Staining schedule

10mins Uranyl acetate

2x 50% ethanol wash

1% distilled H_2O wash

Air dry

10 mins Reynolds Lead citrate in 1M NaOH moistened chamber

2x 1M NaOH

wash distilled H_2O

Air dry

7.3 Oligodendrocyte culture

7.3.1 DMEM 10%

500ml Dulbeccos modified Eagle Medium

5ml Fungizone

5ml 100x Glutamine

2.5ml Gentamycin

50ml Foetal bovine serum

7.3.2 Sato mix

Glucose (1g/L)
BSA Pathocyte (0.0286%)
Progesterone (0.2µM)
Putrescine (0.1µM)
Thyroxine (0.45µM)
Selenite (0.224µM)
Tri-iodothyronine (0.5µM)

7.3.3 Sato conditioned Medium

50ml Dulbeccos modified Eagle Medium containing fungizone and gentamycin
1ml 100x Glutamine
1ml 0.5mg/ml Bovine Insulin
500µl 1% Apo transferrin
50µl Foetal bovine serum
1ml Sato Mix
Mix final 5 ingredients and sterilize through a 0.2µm syringe filter into DMEM.

7.3.4 Stop solution

Soyabean trypsin inhibitor (0.52mg/ml)
Bovine serum albumin factor V (3mg/ml)
DNase (0.04mg/ml)
Make up in HBSS and filter sterilize

7.3.5 Poly-D-Lysine treated dishes

Using sterile technique, 13.3µg/ml Poly L Lysine in sterile distilled water was added to 35mm vented Petri dishes for 30mins. The Poly L Lysine was aspirated and the dishes rinsed once with sterile distilled water then left to dry. Petri dishes were then repackaged for use as required

7.4 Biochemistry and Molecular biology buffers

7.4.1 Tris buffer saline (10x)

12g Tris base

87g sodium chloride

Make up to 800ml adjust to pH7.4 1M HCl top up to 1L

7.4.2 Tris acetate EDTA buffer x10 (TAE buffer)

48.4g Tris base

11.4ml Glacial acetic acid

20ml 0.5M EDTA

Make up to 1L Distilled H_2O

7.4.3 SDS Page Running buffer (10x)

144g Glycine

30.3g Tris

10g SDS

Dissolve glycine then add Tris and finally SDS make up to 1L

7.4.4 Towbin transfer buffers

Anode 1

36g Tris

74ml Methanol

Make up to 1L

Anode 2

3g Tris

75ml Methanol

Make up to 1L

Cathode

3g Glycine

3g Tris

74ml Methanol

Make up to 1L

7.4.5 TBS-T Buffer

100ml Tris Buffer

1ml Tween

7.4.6 Cell Lysis Buffer

1ml 10% Triton x-100

1ml 10x TBS

20µl 0.5M EDTA

5 µl 1M DTT

5 µl 10mg/ml Aprotinin

5 µl 10mg/ml Leupeptin

5 µl 10mg/ml Trypsin inhibitor

100 µl 100mM Benzamidine

100 µl 250mM sodium orthovanadate

100 µl 100mM sodium pyrophosphate

40 µl 250mM PMSF

Make up to 10ml with distilled H_2O Add PMSF immediately before use.

7.4.7 Ponceau S

0.1% Ponceau S powder

1% Glacial acetic acid

7.4.8 Bromo phenol Blue loading Dye (6x)

0.04% Bromophenol Blue
0.04% Xylene cyanol
15% Ficoll 400
500µl 1M Tris-HCl
5ml 0.5M EDTA
Make up to 50ml H_2O

7.4.9 Orange G Loading Dye (6x)

15% Ficoll 400
500µl 1M Tris-HCl
5ml 0.5M EDTA
0.4% Orange G
Make up to 50 ml H_2O

7.4.10 DEPC-treated water

0.1% solution of DEPC was made in distilled water and left for at least 12 hours to inactivate contaminating RNases. The water was autoclaved for 20 minutes to destroy the DEPC before use and stored sealed at room temperature until required.

8. Abbreviations

3XSDS/DDT	3x concentration sodiumdodecylsulphate/dithiothreitol
ABC	Avidin-Biotin complex
ANOVA	one way analysis of variation statistical test
AOI	area of interest
APC	Adenomatous Polyposis Coli
APES	3-aminopropyltriethoxy-silane
ASPA	aspartoacylase
ATF3	Activating transcription factor 3
ATF6	Activating transcription factor 6
BCA	Bichinoic acid
BiP	chaperone protein
BSA	Bovine serum albumin
CC-1	APC directed against CC-1 identifies oligodendrocytes
CD45	CD45 antigen
cDNA	complimentary deoxyribonucleic acid
CNP	2′ ,3′,cyclic nucleotide 3′-phosphodiesterase
CNS	central nervous system
DAB	3,4,3′,4′,-tetraminobiphenyl hydrochloride
DAPI	4′,6-diamidino-2-phenylindole
DDSA	Dodecyl succinic anhydride
DEPC	diethyl pyrocarbonate
dH2O	distilled water
DM20	26.5kDa protein isoform encoded by *Plp* gene
DMEM10%	Dulbeccos modified eagle medium with 10% Foetal calf serum
DMP30	tri-dimethylaminomethyl phenol
DNA	deoxyribonucleic acid
DNase	deoxyribonuclease
DTT	dithiothreitol
ECL	enhanced chemiluminescent substrate
EM	Electron microscopy
ER	Endoplasmic reticulum
ERAD	endoplasmic reticulum associated degradation

ERSE	endoplasmic reticulum stress response element
FAM	fluorescein reporter label for rPCR
FITC	fluorescein isothiocyanate
gDNA	genomic deoxyribonucleic acid
GalC	galactocerebroside
GFAP	glial fibrillary acidic protein
HBSS	Hanks balanced salt solution
IRE1	Inositol requiring enzyme 1
MAG	myelin-associated glycoprotein
Mbp	myelin basic protein gene
MBP	myelin basic protein
MES	2-(N-morpholino)ethanesulfonic acid
MOBP	myelin-associated oligodendrocytic basic protein
MOG	myelin/oligodendrocyte glycoprotein
mRNA	messenger ribonucleic acid
NG2	sulphated proteoglycan
NGS	normal goat serum
OPC	oligodendrocyte progenitor cells
OSP	oligodendrocyte specific protein
P20	postnatal day 20
P40	postnatal day 40
PBS	phosphate buffered saline
PCR	polymerase chain reaction
PDGFR	platelet derived growth factor a receptor
PERK	PKR-like resistant kinase
PLP	proteolipid protein (30kDa protein isoform encoded by *Plp* gene)
P-L-P	periodate-lysine-paraformaldehyde
PLP1	proteolipid protein (human gene)
Plp1	proteolipid protein (non-human gene)
Plp^{jp}	jimpy
$Plp^{jp\text{-}4j}$	jimpy-4j
$Plp^{jp\text{-}msd}$	myelin synthesis deficient
$Plp^{jp\text{-}rsh}$	rumpshaker
Plp^{md}	myelin deficient
Plp^{pt}	paralytic tremor
Plp^{sh}	shaking pup
Plp^{tmkn1}	targeted mutation of the PLP gene

PMD	Pelizaeus-Merzbacher disease
PMSF	phenylmethanesulphonylfluoride
PVDF	polyvinylidene fluoride transfer membrane
qPCR	Quantitative polymerase chain reaction
rRNA	ribosomal ribonucleic acid
RNA	ribonucleic acid
RNase	ribonuclease
rsh	rumpshaker
rshtr	transgene-complemented rumpshaker
RT-PCR	reverse transcription polymerase chain reaction
SDS	sodium dodecyl sulphate
SDS-PAGE	sodium dodecyl sulphate polyacrylamide gel electrophoresis
shi	shiverer
SPG2	Spastic Paraplegia Type 2
SVZ	subventricular zone
TAE	tris acetate ethylene-di-amine-tetra-acetate buffer
TBS	tris buffered saline
TLCK	Na -p-tosyl-l-lysine chloro-methyl ketone
tRNA	transfer ribonucleic acid
TxR	Texas red
UPR	unfolded protein response
UV	ultraviolet
WT	wild type
xbp-1	gene encoding X-Box protein1
XBP-1	X-Box protein 1

Reference List

References

Al-Saktawi K, McLaughlin M, Klugmann M, Schneider A, Barrie JA, McCulloch MC, Montague P, Kirkham D, Nave K-A, Griffiths IR (2003) Genetic background determines phenotypic severity of the *Plp rumpshaker* mutation. J.Neurosci.Res. 72:12-24.

Anderson TJ, Schneider A, Barrie JA, Klugmann M, McCulloch MC, Kirkham D, Kyriakides E, Nave K-A, Griffiths IR (1998) Late-onset neurodegeneration in mice with increased dosage of the proteolipid protein gene. J.Comp.Neurol. 394:506-519.

Barres BA, Barde YA (2000) Neuronal and glial cell biology. Curr.Opin.Neurobiol. 10:642-648.

Baumann N, Pham-Dinh D (2001) Biology of oligodendrocyte and myelin in the mammalian central nervous system. Physiol.Rev. 81:871-927.

Billings-Gagliardi S, Nunnari JN, Nadon NL, Wolf MK (1999) Evidence that CNS hypomyelination does not cause death of jimpy-msd mutant mice. Dev.Neurosci. 21:473-482.

Butt AM, Ibrahim M, Ruge FM, Berry M (1995) Biochemical subtypes of oligodendrocyte in the anterior medullary velum of the rat as revealed by the monoclonal antibody Rip. Glia 14:185-197.

Campagnoni AT, Campagnoni CW (2004) Myelin Basic Protein. In: Myelin Biology and Disorders (Lazzarini RA, Griffin JW, Lassmann H, Nave K-A, Miller RH, Trapp BD eds), pp 387-400. Amsterdam: Elsevier.

Cerghet M, Bessert DA, Nave KA, Skoff RP (2001) Differential expression of apoptotic markers in *jimpy* and in *Plp* overexpressors: evidence for different apoptotic pathways. J.Neurocytol. 30:841-855.

Colognato H, ffrench-Constant C (2004) Mechanisms of glial development. Curr.Opin.Neurobiol. 14:37-44.

Coman L, Barbin G, Charles P, Zalc B, Lubetzki C (2005) Axonal signals in central nervous system myelination, demyelination and remyelination. J.Neurol.Sci. 233:67-71.

Dickinson PJ, Griffiths IR, Barrie JA, Kyriakides E, Pollock GS, Barnett SC, Barrie JM, Pollock GF (1997) Expression of the *dm-20* isoform of the plp gene in olfactory nerve ensheathing cells: evidence from developmental studies. J.Neurocytol. 26:181-189.

Diehl H-J, Schaich M, Budzinski R-M, Stoffel W (1986) Individual exons encode the integral membrane domains of human proteolipid protein. Proc.Natl.Acad.Sci.USA 83:9807-9811.

Edgar JM, Garbern J (2004) The myelinated axon is dependent on the myelinating cell for support and maintenance: molecules involved. J.Neurosci.Res. 76:593-598.

Edgar JM, McLaughlin M, Yool D, Zhang SC, Fowler J, Montague P, Barrie JA, McCulloch MC, Duncan ID, Garbern J, Nave K-A, Griffiths IR (2004) Oligodendroglial modulation of fast axonal transport in a mouse model of hereditary spastic paraplegia. J.Cell Biol. 166:121-131.

Fanarraga ML, Sommer I, Griffiths IR (1995) O-2A progenitors of the mouse optic nerve exhibit a developmental pattern of antigen expression different from the rat. Glia 15:95-104.

Fernandez PA, Tang DG, Cheng LL, Prochiantz A, Mudge AW, Raff MC (2000) Evidence that axon-derived neuregulin promotes oligodendrocyte survival in the developing rat optic nerve. Neuron 28:81-90.

Folch J, Lees M (1951) Proteolipids, a new type of tissue lipoproteins. J.Biol.Chem. 191:807-817.

Garbern JY (2007) Pelizaeus-Merzbacher disease: Genetic and cellular pathogenesis. Cell Mol.Life Sci. 64:50-65.

Gow A (1997) Redefining the lipophilin family of proteolipid proteins. J.Neurosci.Res. 50:659-664.

Gow A (2004) Protein Misfolding as a Disease Determinant. In: Myelin Biology and Disorders (Lazzarini RA, Griffin JW, Lassmann H, Nave K-A, Miller RH, Trapp BD eds), pp 1009-1038. Amsterdam: ELSEVIER.

Griffiths IR, Duncan ID, McCulloch M (1981) Shaking pup: a disorder of central myelination in the spaniel dog. II. Ultrastructural observations on the white matter of cervical spinal cord. J.Neurocytol. 10:847-858.

Griffiths IR, Klugmann M, Anderson TJ, Schwab MH, Jung M, Zimmermann F, Nave K-A (1997) Mouse models of dysmyelinating diseases: axonal degeneration and glial cell death. J.Neurochem. 69:S257(Abstract)

Gülow K, Bienert D, Haas IG (2002) BiP is feed-back regulated by control of protein translation efficiency. J.Cell Sci. 115:2443-2452.

He Y, Appel S, Le WD (2001) Minocycline inhibits microglial activation and protects nigral cells after 6-hydroxydopamine injection into mouse striatum. Brain Res. 909:187-193.

Hudson LD, Garbern JY, Kamholz JA (2004) Pelizaeus-Merzbacher disease. In: Myelin biology and disorders (Lazzarini RA, Griffin JW, Lassmann H, Nave K-A, Miller RH, Trapp BD eds), pp 867-885. Amsterdam: Elsevier.

Inoue K (2005) PLP1-related inherited dysmyelinating disorders: Pelizaeus-Merzbacher disease and spastic paraplegia type 2. Neurogenetics. 6:1-16.

Ip CW, Kroner A, Crocker PR, Nave K-A, Martini R (2006) Sialoadhesin deficiency ameliorates myelin degeneration and axonopathic changes in the CNS of PLP overexpressing mice. Neurobiology of Disease 25:105-111.

Karthigasan J, Evans EL, Vouyiouklis DA, Inouye H, Borenshteyn N, Ramamurthy GV, Kirschner DA (1996) Effects of rumpshaker mutation on CNS myelin composition and structure. J.Neurochem. 66:338-345.

Kimura M, Sato M, Akatsuka A, Nozawa-Kimura S, Takahashi R, Yokoyama M, Nomura T, Katsuki M (1989) Restoration of myelin formation by a single type of myelin basic protein in transgenic shiverer mice. Proc.Natl.Acad.Sci.USA 86:5661-5665.

Kramer-Albers EM, Gehrig-Burger K, Thiele C, Trotter J, Nave KA (2006) Perturbed interactions of mutant proteolipid protein/DM20 with cholesterol and lipid rafts in oligodendroglia: implications for dysmyelination in spastic paraplegia. J.Neurosci. 26:11743-11752.

Lappe-Siefke C, Goebbels S, Gravel M, Nicksch E, Lee J, Braun PE, Griffiths IR, Nave K-A (2003) Disruption of the *CNP* gene uncouples oligodendroglial functions in axonal support and myelination. Nat.Genet. 33:366-374.

Lee AH, Iwakoshi NN, Glimcher LH (2003) XBP-1 regulates a subset of endoplasmic reticulum resident chaperone genes in the unfolded protein response. Mol Cell Biol 23:7448-7459.

Lin W, Harding HP, Ron D, Popko B (2005) Endoplasmic reticulum stress modulates the response of myelinating oligodendrocytes to the immune cytokine interferon-gamma. J.Cell Biol. 169:603-612.

Macklin WB, Campagnoni AT, Deininger PL, Gardinier MV (1987) Structure and expression of the mouse proteolipid protein gene. J.Neurosci.Res. 18:383-394.

Marciniak SJ, Yun CY, Oyadomari S, Novoa I, Zhang YH, Jungreis R, Nagata K, Harding HP, Ron D (2004) CHOP induces death by promoting protein synthesis and oxidation in the stressed endoplasmic reticulum. Genes Dev. 18:3066-3077.

McLaughlin M, Barrie JA, Karim SA, Montague P, Edgar JM, Kirkham D, Thomson CE, Griffiths IR (2006) Processing of PLP in a model of Pelizaeus-Merzbacher disease/SPG2 due to the *rumpshaker* mutation. Glia 53:715-722.

McLaughlin M, Karim SA, Montague P, Barrie JA, Kirkham D, Griffiths IR, Edgar JM (2007) Genetic background influences UPR but not PLP processing in the *rumpshaker* model of PMD/SPG2. Neurochem.Res 32:167-176.

McTigue DM, Wei P, Stokes BT (2001) Proliferation of NG2-positive cells and altered oligodendrocyte numbers in the contused rat spinal cord. J.Neurosci. 21:3392-3400.

Meyer-Franke A, Shen SL, Barres BA (1999) Astrocytes induce oligodendrocyte processes to align with and adhere to axons. Mol.Cell.Neurosci. 14:385-397.

Miller MJ, Haxhiu MA, Georgiadis P, Gudz TI, Kangas CD, Macklin WB (2003) Proteolipid protein gene mutation induces altered ventilatory response to hypoxia in the myelin-deficient rat. J.Neurosci. 23:2265-2273.

Milner RJ, Lai C, Nave K-A, Lenoir D, Ogata J, Sutcliffe JG (1985) Nucleotide sequence of two mRNAs for rat brain myelin proteolipid protein. Cell 42:931-939.

Momoi T (2004) Caspases involved in ER stress-mediated cell death. J.Chem.Neuroanat. 28:101-105.

Mori S, Leblond CP (1970) Electron microscopic identification of three classes of oligodendrocytes and a preliminary study of their proliferative activity in the corpus callosum of young rats. J.Comp.Neurol. 139:1-30.

Nadon NL, Arnheiter H, Hudson LD (1994) A combination of PLP and DM20 transgenes promotes partial myelination in the jimpy mouse. J.Neurochem. 63:822-833.

Naidu S, Dlouhy SR, Geraghty MT, Hodes ME (1997) A male child with the *rumpshaker* mutation, X-linked spastic paraplegia Pelizaeus-Merzbacher disease and lysinuria. J.Inherited Metab.Dis. 20:811-816.

Nave K-A, Griffiths IR (2004) Models of Pelizaeus-Merzbacher disease. In: Myelin biology and disorders (Lazzarini RA, Griffin JW, Lassmann H, Nave K-A, Miller RH, Trapp BD eds), pp 1125-1142. Amsterdam: Elsevier.

Nedergaard M, Ransom B, Goldman SA (2003) New roles for astrocytes: Redefining the functional architecture of the brain. Trends Neurosci. 26:523-530.

Oyadomari S, Mori M (2004) Roles of CHOP/GADD153 in endoplasmic reticulum stress. Cell Death Differ. 11:381-389.

Rao RV, Ellerby HM, Bredesen DE (2004) Coupling endoplasmic reticulum stress to the cell death program. Cell Death Differ. 11:372-380.

Readhead C, Popko B, Takahashi N, Shine HD, Saavedra RA, Sidman RL, Hood L (1987) Expression of a myelin basic protein gene in transgenic shiverer mice: correction of the dysmyelinating phenotype. Cell 48:703-712.

Readhead C, Schneider A, Griffiths IR, Nave K-A (1994) Premature arrest of myelin formation in transgenic mice with increased proteolipid protein gene dosage. Neuron 12:583-595.

Schneider A, Lander H, Schulz G, Wolburg H, Nave KA, Schulz JB, Simons M (2005) Palmitoylation is a sorting determinant for transport to the myelin membrane. J Cell Sci. 118:2415-2423.

Schneider A, Montague P, Griffiths IR, Fanarraga ML, Kennedy PGE, Brophy PJ, Nave K-A (1992) Uncoupling of hypomyelination and glial cell death by a mutation in the proteolipid protein gene. Nature 358:758-761.

Schwab ME, Schnell L (1989) Region-specific appearance of myelin constituents in the developing rat spinal cord. J.Neurocytol. 18:161-169.

Seiwa C, Sugiyama I, Yagi T, Iguchi T, Asou H (2000) Fyn tyrosine kinase participates in the compact myelin sheath formation in the central nervous system. Neurosci.Res. 37:21-31.

Sharma R, Jiang HY, Zhong L, Tseng J, Gow A (2007) Minimal role for activating transcription factor 3 in the oligodendrocyte unfolded protein response in vivo. J.Neurochem. (In Press)

Shine HD, Readhead C, Popko B, Hood L, Sidman RL (1992) Morphometric analysis of normal, mutant and transgenic CNS: correlation of myelin basic protein expression to myelinogenesis. J.Neurochem. 58:342-349.

Simons M, Krämer EM, Thiele C, Stoffel W, Trotter J (2000) Assembly of myelin by association of proteolipid protein with cholesterol- and galactosylceramide-rich membrane domains. J.Cell Biol. 151:143-153.

Skoff RP (1995) Programmed cell death in the dysmyelinating mutants. Brain Pathol. 5:283-288.

Skoff RP, Saluja I, Bessert D, Yang X (2004) Analyses of proteolipid protein mutants show levels of proteolipid protein regulate oligodendrocyte number and cell death *in vitro* and *in vivo*. Neurochem.Res. 29:2095-2103.

Southwood CM, Garbern J, Jiang W, Gow A (2002) The unfolded protein response modulates disease severity in Pelizaeus- Merzbacher disease. Neuron 36:585-596.

Southwood CM, Peppi M, Dryden S, Tainsky MA, Gow A (2006) Microtubule Deacetylases, SirT2 and HDAC6, in the Nervous System. Neurochem.Res (In Press)

Stevens B (2003) Glia: much more than the neuron's side-kick. Curr.Biol. 13:R469-R472

Tetzloff SU, Bizzozero OA (1998) Palmitoylation of proteolipid protein from rat brain myelin using endogenously generated ^{18}O-fatty acids. J.Biol.Chem. 273:279-285.

Thomson CE, Anderson TJ, McCulloch MC, Dickinson PJ, Vouyiouklis DA, Griffiths IR (1999) The early phenotype associated with the jimpy mutation of the proteolipid protein gene. J.Neurocytol. 28:207-221.

Trajkovic K, Dhaunchak AS, Goncalves JT, Wenzel D, Schneider A, Bunt G, Nave KA, Simons M (2006) Neuron to glia signaling triggers myelin membrane exocytosis from endosomal storage sites. J.Cell Biol. 172:937-948.

Trapp BD, Pfeiffer S, Anitei M, Kidd GJ (2004) Cell Biology of Myelin Assembly. In: Myelin Biology and Disorders (Lazzarini RA, Griffin JW, Lassmann H, Nave K-A, Miller RH, Trapp BD eds), pp 29-55. Amsterdam: Elsevier.

Umemori H, Kadowaki Y, Hirosawa K, Yoshida Y, Hironaka K, Okano H, Yamamoto T (1999) Stimulation of myelin basic protein gene transcription by Fyn tyrosine kinase for myelination. J.Neurosci. 19:1393-1397.

Vilhardt F (2005) Microglia: phagocyte and glia cell. Int.J.Biochem.Cell Biol. 37:17-21.

Vouyiouklis DA, Barrie JA, Griffiths IR, Thomson CE (2000) A proteolipid protein-(PLP)-specific pre-mRNA contains intron 3 and is upregulated during myelination in the CNS. J.Neurochem. 74:940-948.

Werner HB, Kuhlmann K, Shen S, Uecker M, Schardt A, Dimova K, Orfaniotou F, Dhaunchak A, Brinkmann BG, Mobius W, Guarente Ly, Casaccia-Bonnefil P, Jahn O, Nave K-A (2007) Proteolipid Protein Is Required for Transport of Sirtuin 2 into CNS Myelin. J.Neurosci. 27:7717-7730.

Williams MA (1977) Stereological techniques. In: Practical Methods in Electron Microscopy. Vol. 6. Quantitative Methods in Biology (Glauert AM ed), pp 5-84. Amsterdam: North Holland.

Wolf MK, Nunnari JN, Billings-Gagliardi S (1999) Quaking*shiverer double-mutant mice survive for at least 100 days with no CNS myelin. Dev.Neurosci. 21:483-490.

Yool D, Klugmann M, Barrie JA, McCulloch MC, Nave K-A, Griffiths IR (2002) Observations on the structure of myelin lacking the major proteolipid protein. Neuropath.Appl.Neurobiol. 28:75-78.

Yool DA, Edgar JM, Montague P, Malcolm S (2000) The *proteolipid* protein gene and myelin disorders in man and animal models. Hum.Mol.Genet. 9:987-992.

Yoshida H, Oku M, Suzuki M, Mori K (2006) pXBP1(U) encoded in XBP1 pre-mRNA negatively regulates unfolded protein response activator pXBP1(S) in mammalian ER stress response. J.Cell Biol. 172:565-575.